Electronic Supplementary Material (ESI) for Environmental Science: Nano.

Supplementary Information For:

Superhydrophobic Nanosized Metal-Organic Framework Composites for the Targeted Removal of Hydrophobic Pharmaceuticals and Outstanding Bacterial Anti-Adhesion

*Subhrajyoti Ghosh, Abhijeet Rana,[†] Anjali Patel, [†] Debasis Manna, and Shyam Biswas**

Department of Chemistry, Indian Institute of Technology Guwahati, 781039 Assam, India

[†]Equal contribution

*Corresponding author. Tel: 91-3612583309, Fax: 91-3612582349

E-mail address: sbiswas@iitg.ac.in

Materials and General Methods:

All the reagents and solvents were purchased from commercial sources and used without purification, 2-(2,2,3,3,4,4,5,5,6,6,7,7,8,8,8-pentadecafluorooctanamido)threphthalic acid linker (**H_2L**) which was prepared according to the below mentioned procedure. The cotton piece was purchased from Amazon India. The Attenuated Total Reflectance Infrared (ATR-IR) spectra were recorded using PerkinElmer UATR Two at the ambient condition in the region 400-4000 cm^{-1}. The notations used for characterization of the bands are broad (br), strong (s), very strong (vs), medium (m), weak (w) and shoulder (sh). Thermogravimetric analysis (TGA) was carried out with a Netzsch STA-409CD thermal analyzer in the temperature range of 25-800 °C in an O_2 atmosphere at the rate of 5 °C min^{-1}. PXRD data were collected by using Rigaku Smartlab X-ray diffractometer with Cu-K_α radiation (l = 1.54056 Å), 40 kV of operating voltage and 125 mA of operating current. N_2 sorption isotherms were recorded by using Quantachrome Quadrasorb evo volumetric gas adsorption equipment at −196 °C. Before the sorption analysis, the degassing of the compound was carried out at 100 °C under a high vacuum for 12 h. Gemini 500 was utilized for Energy Dispersive X-rays spectrometer (EDX) for elemental characterization. FE-SEM images were captured with a Zeiss (Zemini) scanning electron microscope. JEOL, 2100F Field Emission Transmission electron microscope was used for the collection of FE-TEM images. XPS work was performed with PHI-5000 Versaprobe III (ULVAC-PHI Inc.) using He(I) (21.22 eV) excitation. Pawley refinement was carried out using Materials Studio software. The DICVOL program incorporated within STOE's WinXPow software package was used to determine the lattice parameters. The contact angle measurements were performed by employing a KRUSS Drop Shape Analyzer-DSA-25 instrument with an automatic liquid dispenser at ambient temperature.

Procedure for Absorption of Hydrophobic Drug Molecules by SH-MOF′:

For the sorption study, a 10^4 ppm stock solution of both analytes was prepared in 1:9 mixtures of water and methanol. For the measurement of absorption capacity, different concentrations of solutions of both analytes were prepared using stock solutions. After that, 10 mg of **SH-MOF′** MOF powder was added to 1 mL of the solutions of the analytes and it was allowed to stir for 5 min. After the completion of 5 min, it was centrifuged for 10 min for the complete settle down of the MOF particles. Finally, the absorbance of the solutions was measured by UV-spectrometry and the absorbed amount was calculated using the formula $Q_e = \frac{(C_0 - C_e)V}{m}$. In the equation Q_e is the absorption capacity (mg/g) of the MOF, V (mL) is the volume of analyte solution used, C_e and C_0 (mg/L) are the concentrations of the analyte at equilibrium and before the absorption, respectively and 'm' (mg) is the mass of the used MOF.

The flux for separation of different drug molecules was calculated using the formula: Flux = V/A × T (where V = volume of separated drug molecules, A = area of the composite and T = time required for the separation of drug).

Procedure for Examination of Anti-Adhesive and Bactericidal Properties of SH-MOF′@Cotton and Ag@SH-MOF′@Cotton Composites:

Anti-adhesive and bactericidal effects of nanoparticle and superhydrophobic coating on the fabric were investigated by the adherence propensity of the bacterial cells against *Staphylococcus aureus* (*S. aureus*, MTCC 96). The glycerol stock of the bacterial culture was plated on brain heart infusion (BHI) agar media and incubated for 16-20 h. A single colony from the plate was further inoculated into BHI broth media and was incubated at 37 °C with 180 rpm till its logarithmic phase. The *S. aureus* cells were cultured as mentioned above, and at 10^6 CFU/mL, 1 mL of culture was aliquoted into the sterile tubes. Small pieces of the coated and uncoated fabrics were dipped into culture media tubes, and the tubes were kept for swirling in a shaker incubator at 180 rpm for 2 h for homogenization. Fabric pieces were washed with buffer twice to detach the loosely attached bacterial cells, and they were transferred into another sterile tube with buffer. The mechanical force was given to the sample by sonication for 1 min to detach the strongly adsorbed cells on the fabric. The buffer in the media, which had strongly attached bacterial cells on the fabric, was diluted up to 10 times, and it was spread on the agar plate. The plate was incubated at 37 °C for 16-20 h followed by colony counting from the plate.

FE-SEM Analysis of Bacterial Culture Treated Fabrics:

The *S. aureus* bacterial cells were cultured, as mentioned in the earlier section. Bacterial cells were harvested and re-suspended in PBS buffer. Small pieces of the coated and uncoated fabrics were immersed in bacterial culture. The samples were incubated at 37 °C with 180 rpm in shaking condition for 1 h. Followed by incubation, the fabric was separated from the bacterial culture and washed with buffer to sweep away the loosely attached bacterial cells. Then, 3% glutaraldehyde solution was added to the sample for cell fixation and incubated for 30 min. Glutaraldehyde-containing buffer aspired from the sample, and the fabric was placed in an incubator and allowed to dry at 37 °C. The sample was placed on the FE-SEM grid, and analysis was performed after coating.

Procedure for Synthesis of H_2L Linker:

For the synthesis of H_2L linker, in a two-necked round bottom flux (containing 15 mL of dry THF), 182 mg (1 mmol) of 2-aminoterephthalic acid was added and it was dissolved by sonication. Thereafter, 250 µL (1 mmol) of 2,2,3,3,4,4,5,5,6,6,7,7,8,8,8-pentadecafluorooctanoyl chloride was dropwise added to the aforementioned mixture under stirring condition at room temperature. After the injection of 250 µL of 2,2,3,3,4,4,5,5,6,6,67,7,8,8,8-pentadecafluorooctanoyl chloride, the mixture was stirred for 2 h at room temperature under N_2 atmosphere (Scheme S1). After 2 h, a white colour precipitated appeared. Then, the solvent was evaporated and the obtained white colour product was dried for 12 h in an 80 °C oven. Yield: 520 mg (0.93 mmol, 93%). ^{1}H NMR (500 MHz, DMSO-d_6): δ = 12.62 (s, 1H), 8.83 (d, 1H), 8.13 (d, 1H), 7.86 (d, 1H) ppm. ^{13}C NMR (125 MHz, DMSO-d_6): δ = 168.93, 168.90, 166.05, 155.09, 154.87, 154.66, 137.58, 137.51,

135.72, 135.70, 131.68, 131.49, 126.10, 126.03, 122.76, 122.52, 121.79, 118.04, 117.77, 115.48, 114.74, 112.73, 112.44, 112.16, 110.59, 110.49, 110.30, 110.28, 110.05, 108.46, 108.22, 108.07, 107.88, 107.86, 107.76 ppm. ^{19}F NMR -80.23, -118.85, -118.88, -118.90, -119.23, -119.26, -121.39, -121.78, -122.23, -122.53, -125.77. MALDI-TOF (m/z): 578.20 for $(M+H)^+$ ion (M = mass of **H_2L** linker). In Figures S1-S4, the NMR and mass spectra of the **H_2L** linker are shown.

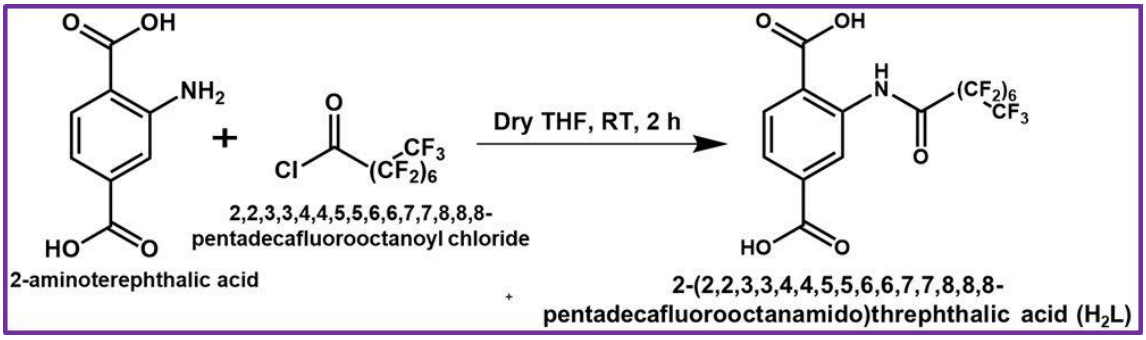

Scheme S1. Reaction scheme for the synthesis of **H_2L** linker.

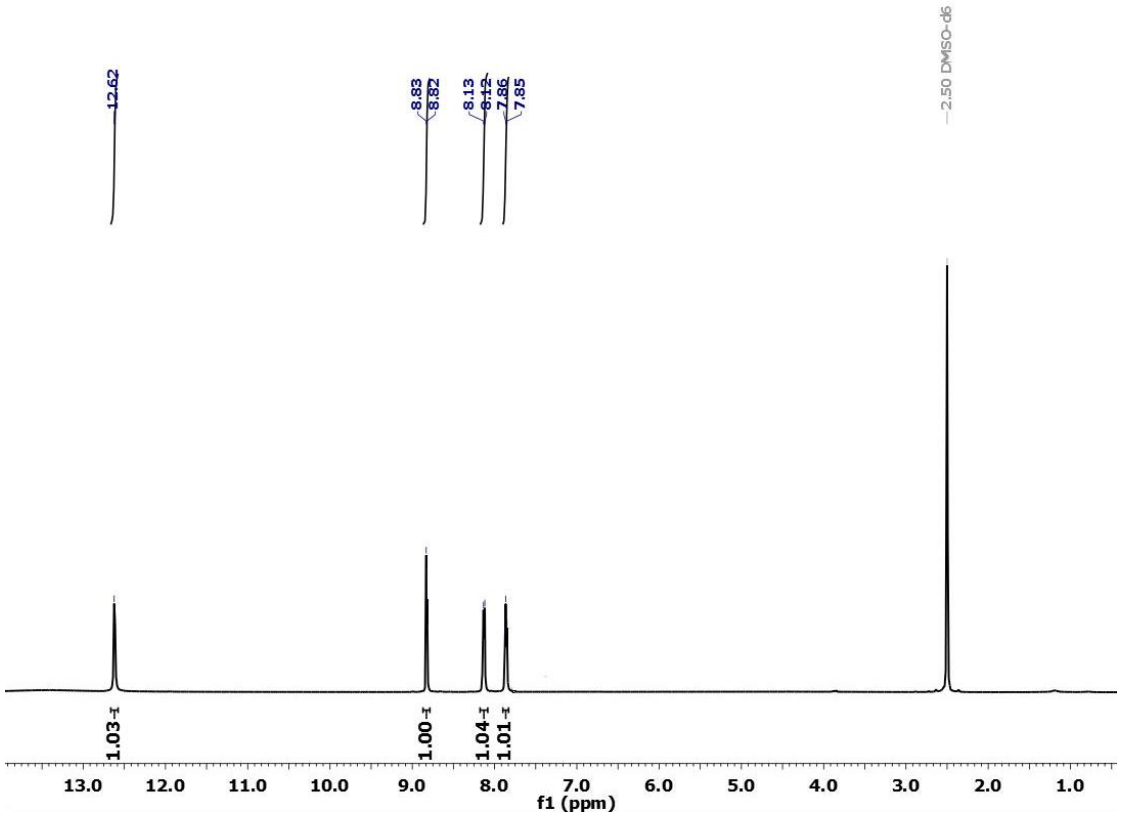

Figure S1. ^{1}H NMR spectrum of **H_2L** linker in DMSO-d_6.

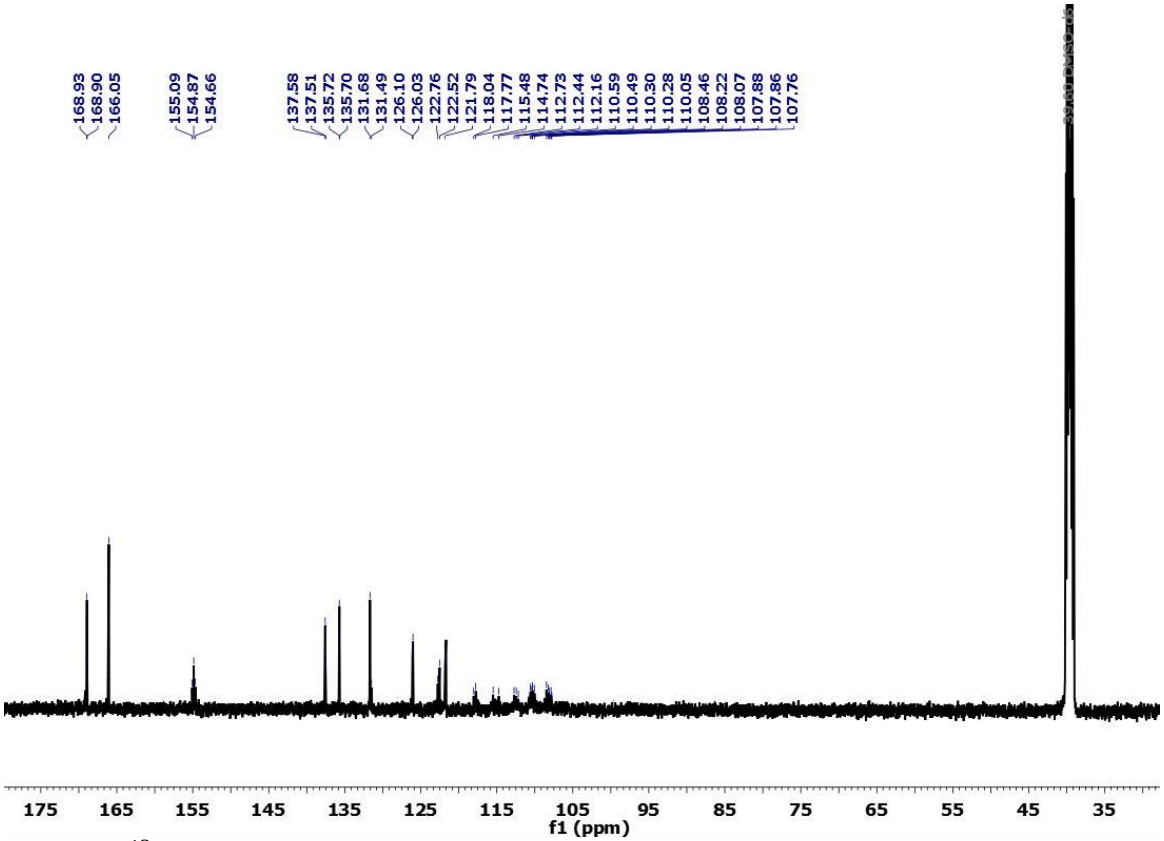

Figure S2. ^{13}C NMR spectrum of **H_2L** linker in DMSO-d_6.

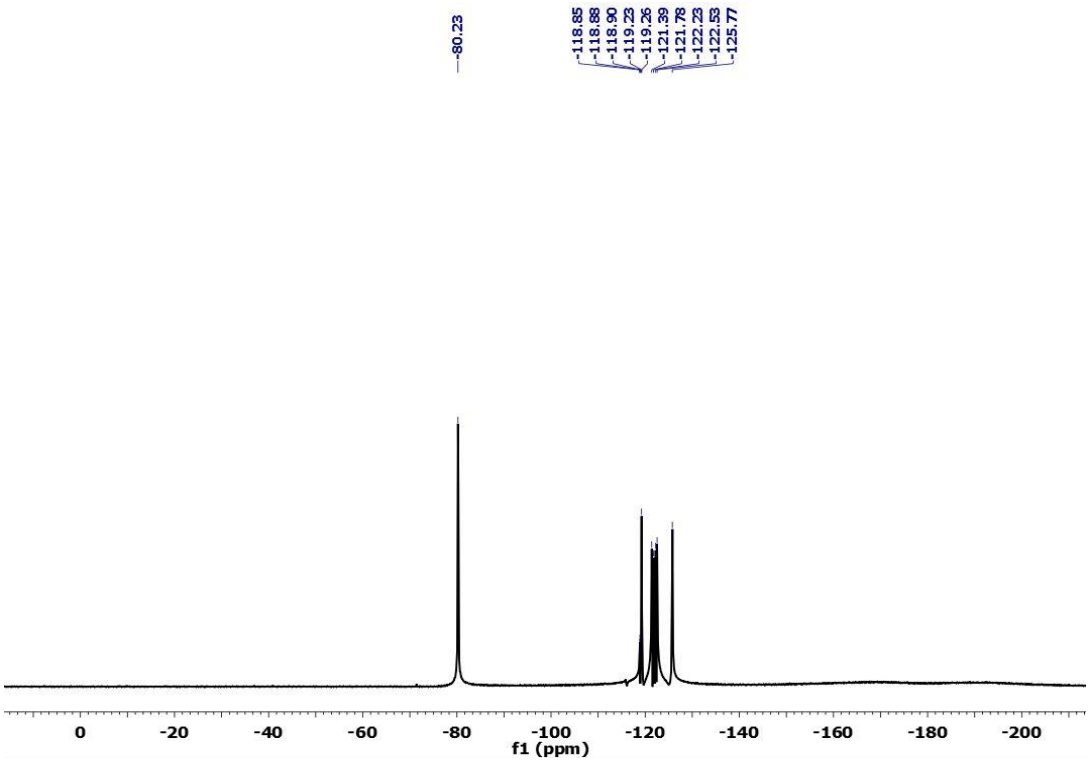

Figure S3. ^{19}F NMR spectrum of **H_2L** linker in DMSO-d_6.

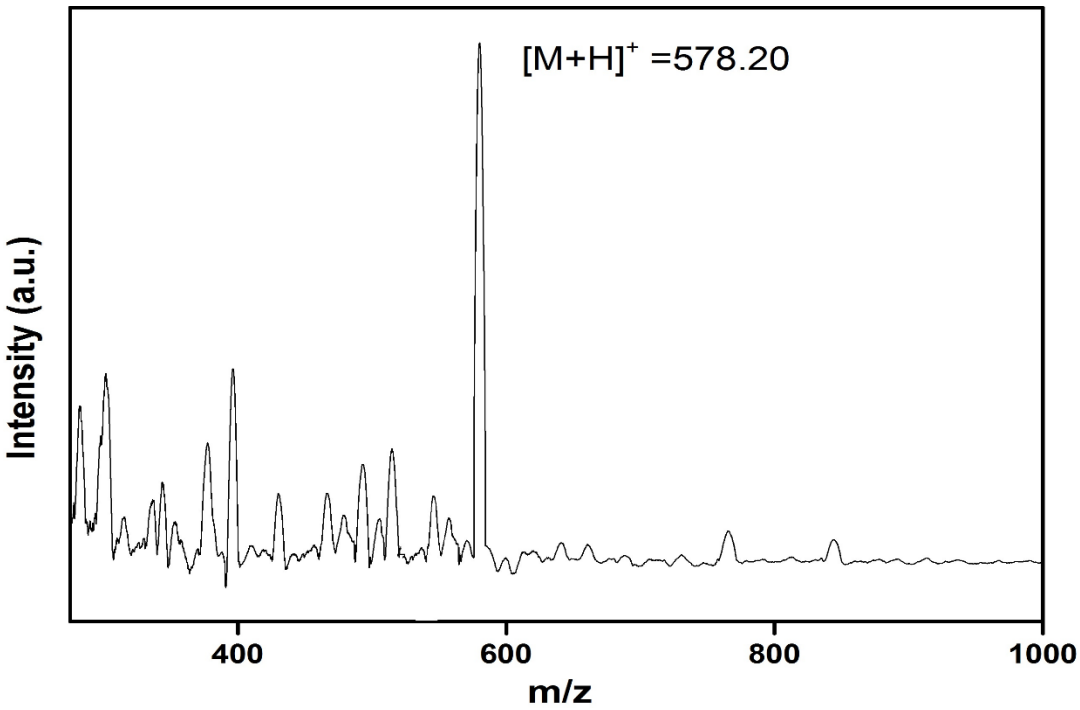

Figure S4. MALDI-TOF mass spectrum of **H_2L** linker measured in methanol. The spectrum shows m/z peak at 578.20, which corresponds to $(M+H)^+$ ion (M = mass of **H_2L** linker).

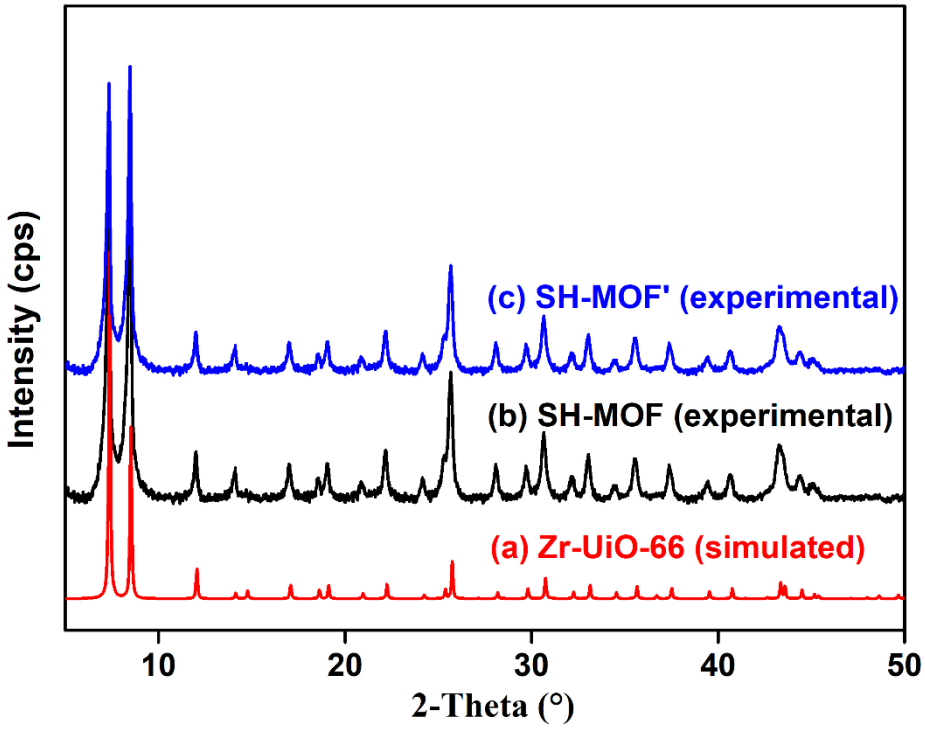

Figure S5. PXRD patterns of (a) Zr-UiO-66 (red), (b) **SH-MOF** (black) and (c) **SH-MOF′** (blue).

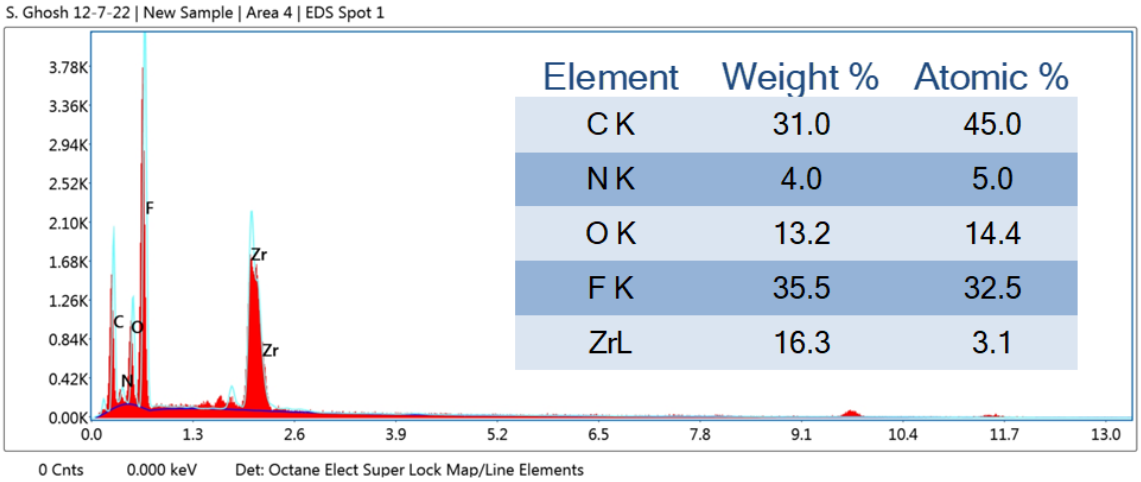

Element	Weight %	Atomic %
C K	31.0	45.0
N K	4.0	5.0
O K	13.2	14.4
F K	35.5	32.5
ZrL	16.3	3.1

Figure S6. EDX spectrum of **SH-MOF′**.

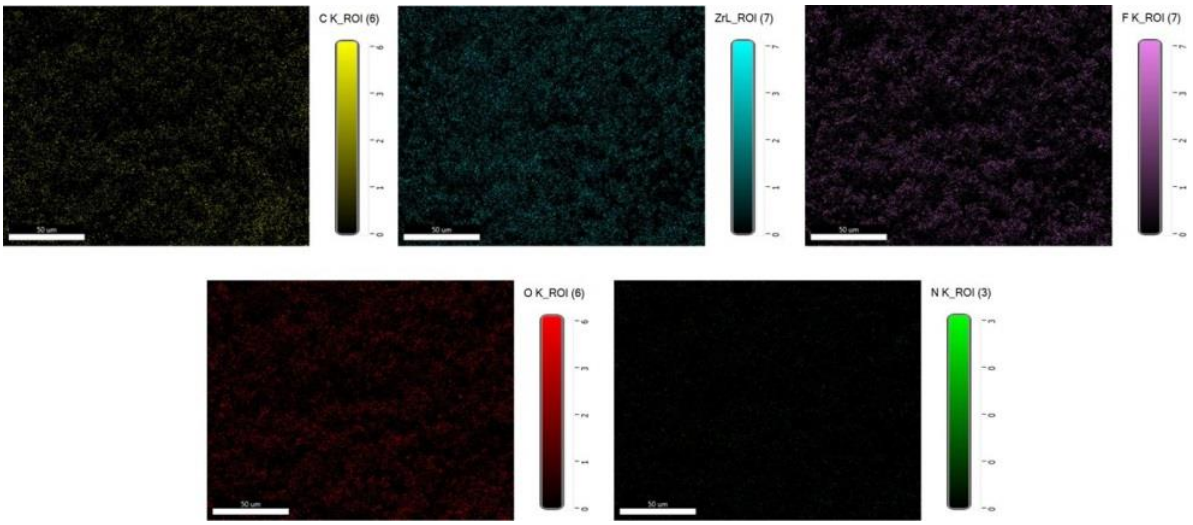

Figure S7. EDX elemental mapping of **SH-MOF′**.

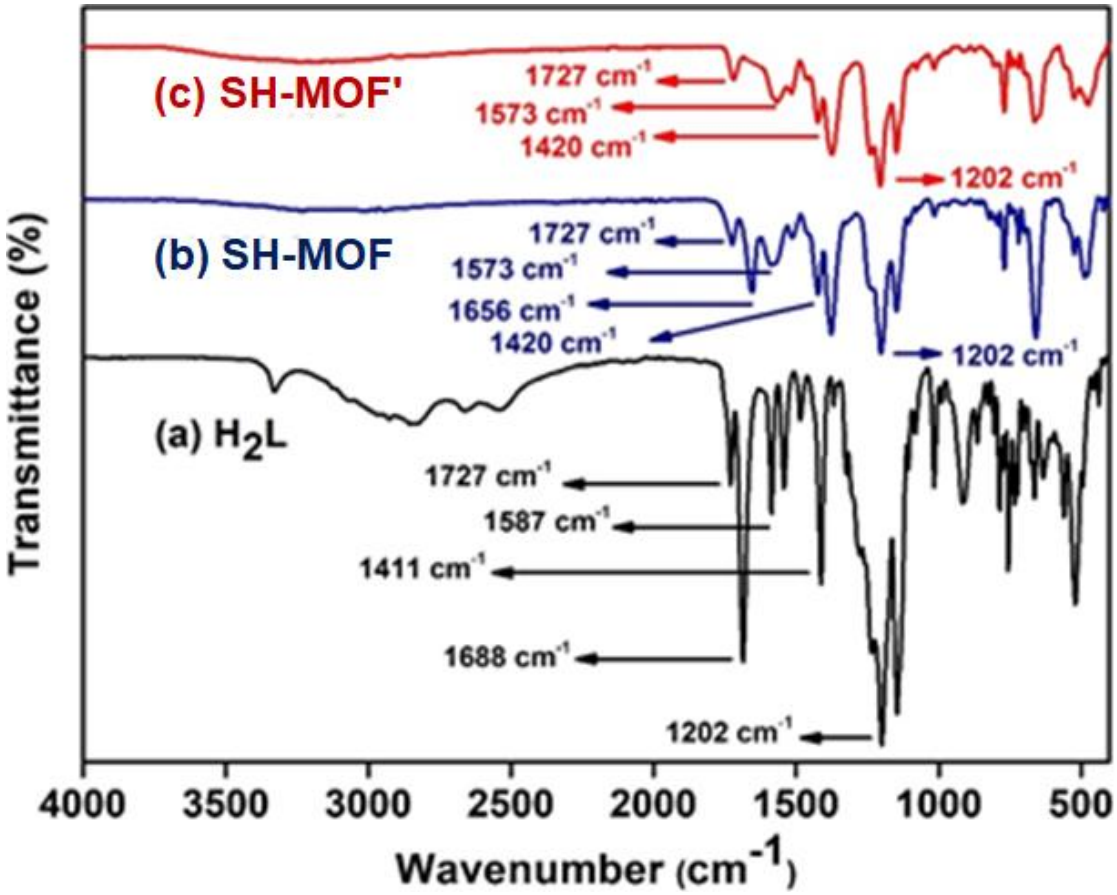

Figure S8. ATR-IR spectra of (a) **H_2L** linker, (b) **SH-MOF** and (c) **SH-MOF′**.

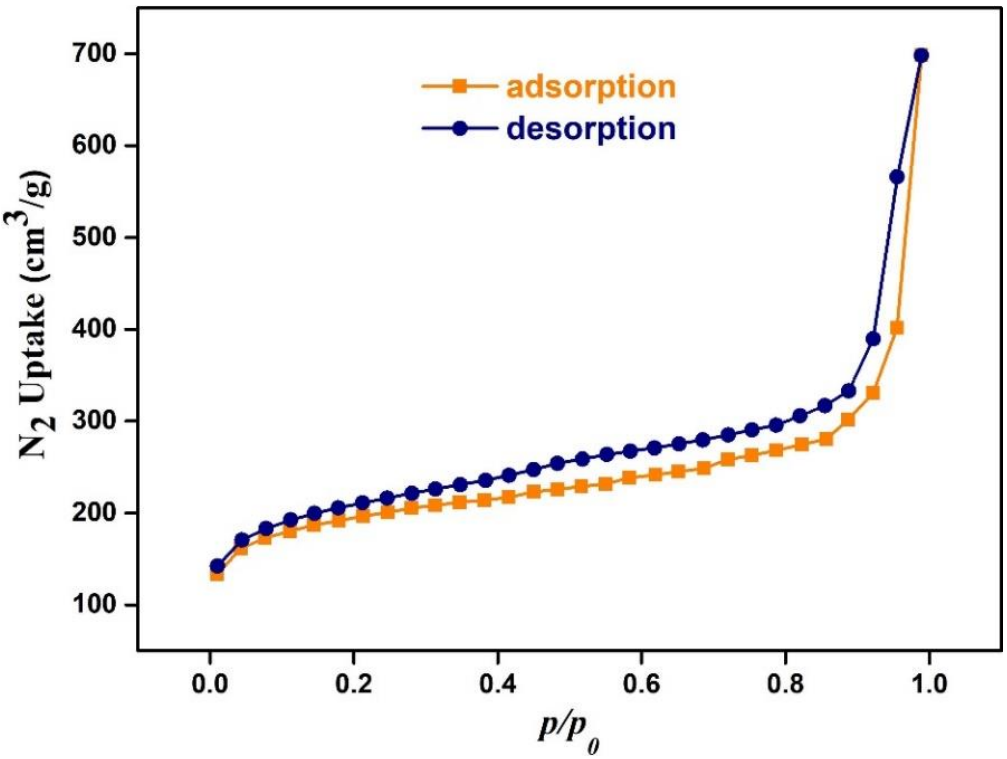

Figure S9. Nitrogen adsorption and desorption isotherms of **SH-MOF′** recorded at –196 °C.

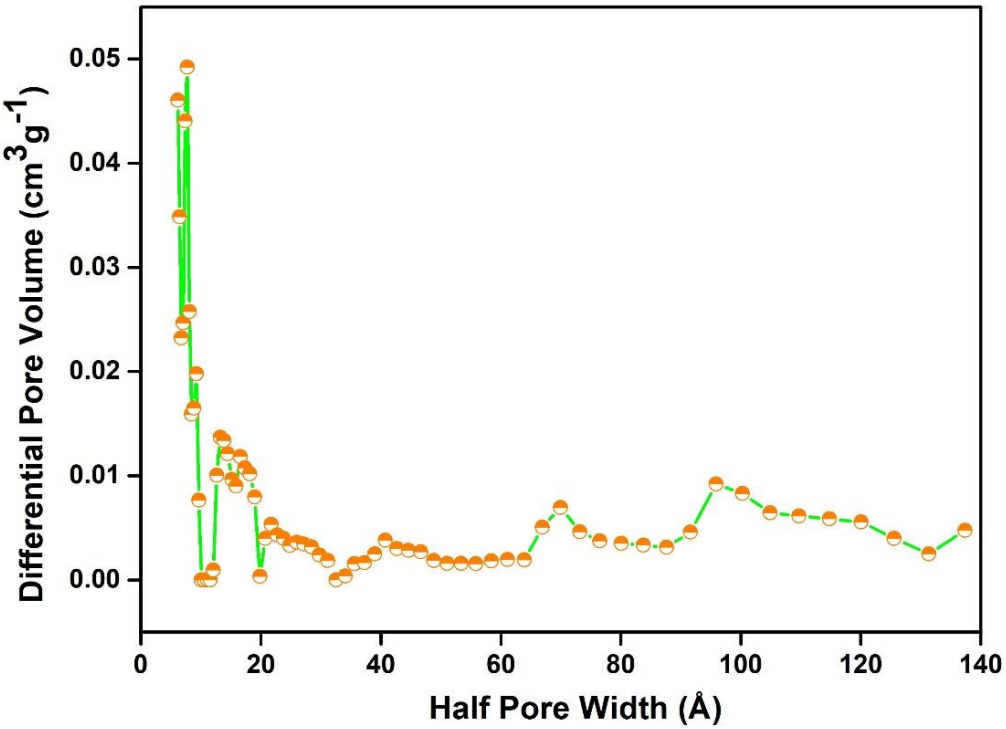

Figure S10. Density functional theory pore-size distribution of compound **SH-MOF′** as determined from its N_2 adsorption isotherms at -196 °C.

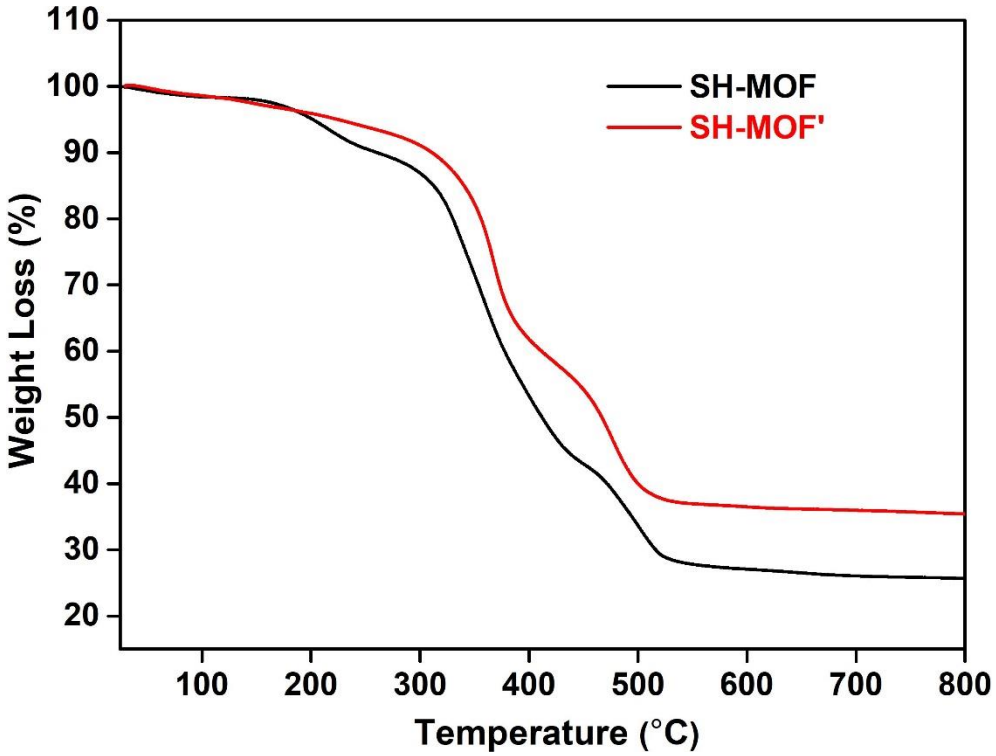

Figure S11. TGA curves of **SH-MOF** (black) and activated **SH-MOF′** (red) recorded in O_2 atmosphere in the temperature range of 25-800 °C at a heating rate of 5 °C min^{-1}.

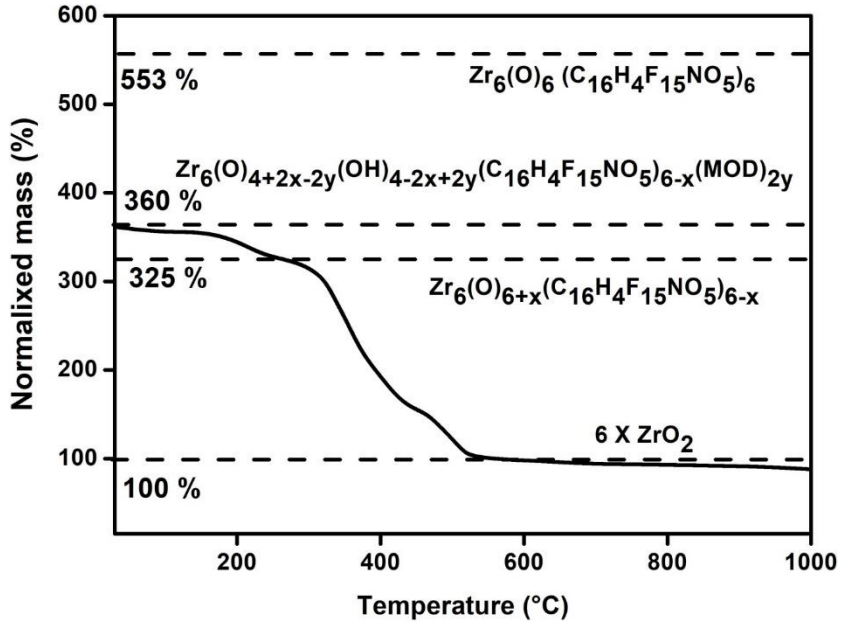

Figure S12. Calculation of missing ligand defects from the TG curve of activated **SH-MOF′**. The vertical dashed line pinpoints $T_{Plat.}$, the temperature at which the plateau ($W_{Exp.\ Plat.}$) is reached. The horizontal dashed lines pinpoint the relevant TGA plateaus.

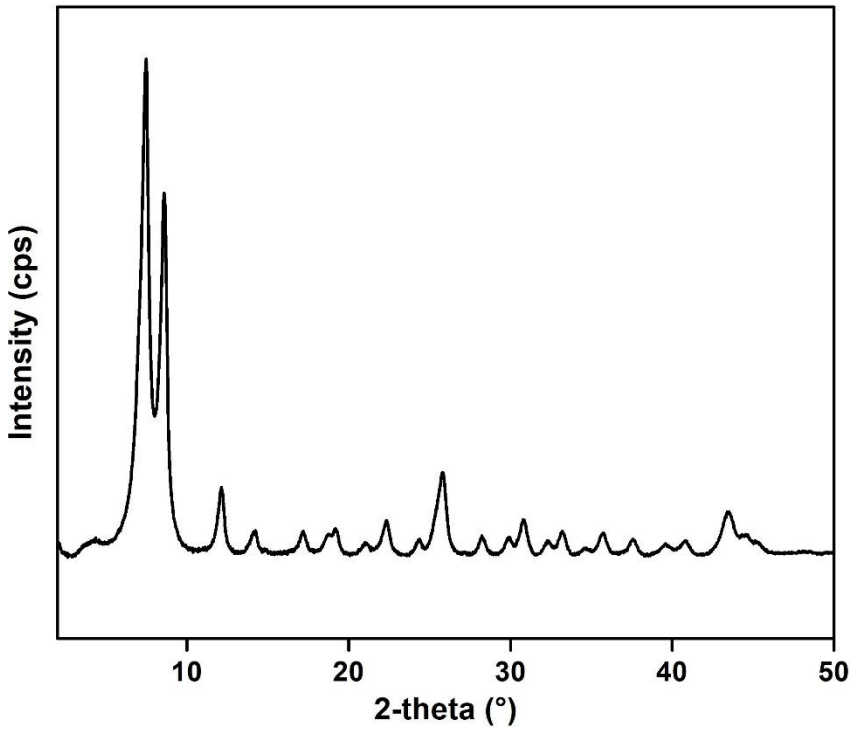

Figure S13. Low angle (2θ <3°) region of the PXRD patterns of **SH-MOF′**.

Calculation of Linker Defects for SH-MOF from TGA Data:

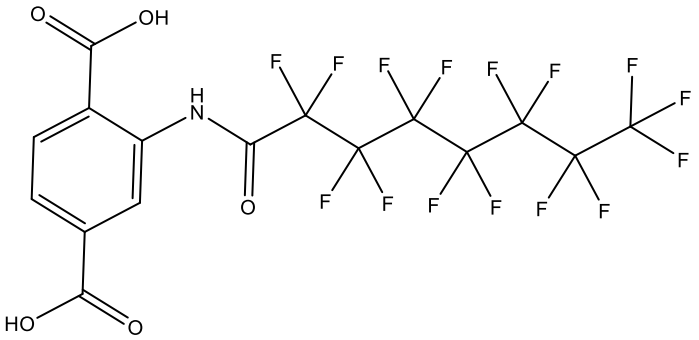

2-(2,2,3,3,4,4,5,5,6,6,7,7,8,8,8-pentadecafluorooctanamido)threphthalic acid linker

Molecular weight = 577.2

Formula of MOF = $Zr_6(O)_4(OH)_4(C_{16}H_4F_{15}NO_5)_6$

Molecular weight = 4130.5 g/mol

- The dehydroxylated and modulator free formula of MOF is $Zr_6(O)_6(C_{16}H_4F_{15}NO_5)_6$ (ideal), Molecular Weight = 4094.4 g/mol
- The dehydroxylated and modulator free formula of MOF is $Zr_6(O)_{6+x}(C_{16}H_4F_{15}NO_5)_{6-x}$ (experimental), Molecular Weight = 4094.4 g/mol (x = number of linker defect)
- From TGA data, after final weight loss step, the remaining mass is due to 6 moles of ZrO_2 i.e. 6 × 123.2 = 739.3 g/mol.
- The ideal weight of $Zr_6(O)_6(C_{16}H_4F_{15}NO_5)_6$ is 5.54 times of 6 moles of ZrO_2
- The remaining flat mass obtained at the last mass on TGA curve was normalized to 100 %.
- The ideal normalized mass percentage for $Zr_6(O)_6(C_{16}H_4F_{15}NO_5)_6$ is 553.7 %.
- The experimental normalized mass percentage of $Zr_6(O)_{6+x}(C_{16}H_4F_{15}NO_5)_{6-x}$ from TGA is 325 %.
- $x = 6 – (W_{wt.\ Plat} - W_{end}/Wt.PL._{Theo})$.

where

- $W_{wt.\ Plat}$ is the (normalized) weight of the sample at the second TGA plateau
- W_{end} is 100 %
- $Wt.PL._{Theo} = (W_{wt.\ ideal\ Plat.} – W_{end})/NL_{ideal}$
- NL_{ideal} = number of linkers per unit formula ideally (6)
- $Wt.PL._{Theo}$ = ((553 7-100)/6) = 76.5 %

- x = 6 - ((325 – 100)/76.5) = 6 – 2.98 = 3
- Number of linker defect per unit formula is 3.

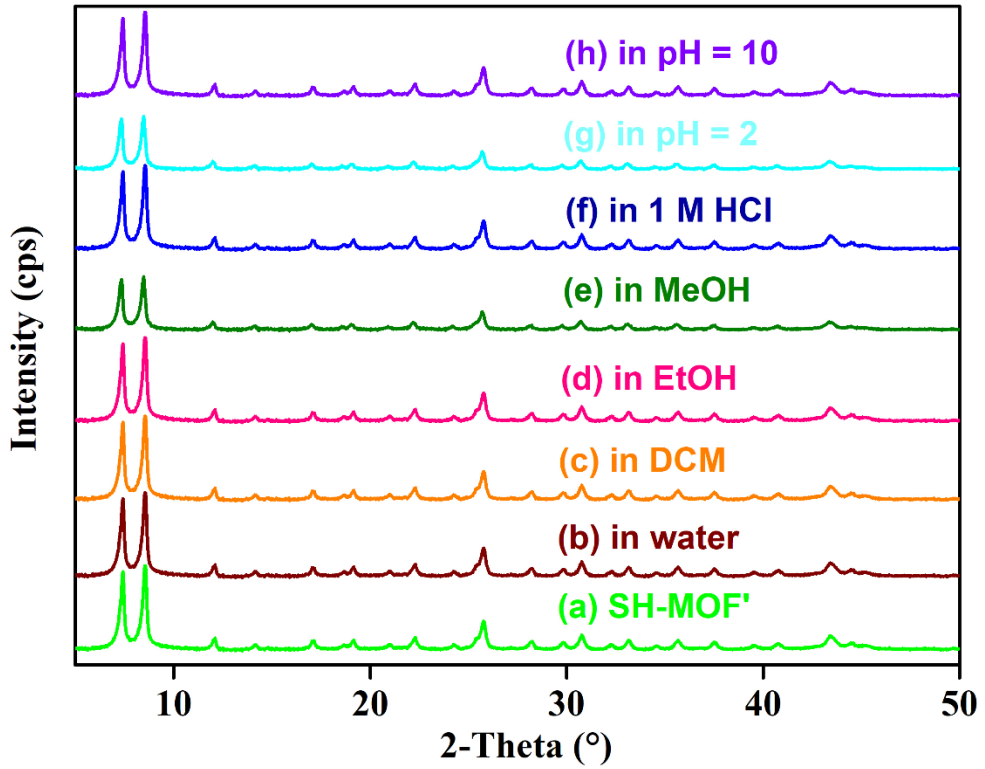

Figure S14. PXRD patterns of (a) **SH-MOF′**, and **SH-MOF′** after stirring in (b) water, (c) DCM, (d) EtOH, (e) MeOH, (f) 1 M HCl, (g) pH = 2 and (f) pH = 10 for 24 h at room temperature.

Table S1. Water Contact angle (WCA) of **SH-MOF′** after treatment with different types of water and solvents.

Liquids	Average WCA of **SH-MOF′ (°)**
Fresh **SH-MOF′**	157 ± 1.0
Water	157 ± 1.2
DCM	156 ± 1.5
EtOH	155 ± 1.0
MeOH	155 ± 1.2
1M HCl	157 ± 1.4
pH = 2	156 ± 1.3
pH = 10	157 ± 1.2

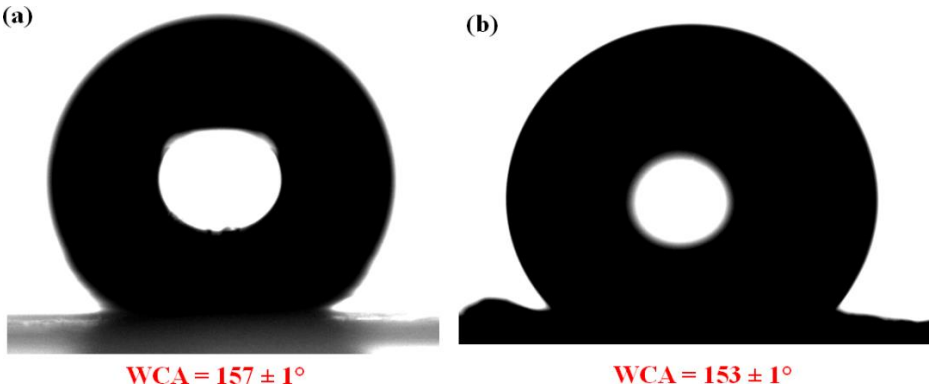

Figure S15. The contact angle image of beaded water droplets on the surface of (a) **SH-MOF′** and (b) **SH-MOF′@cotton** composite.

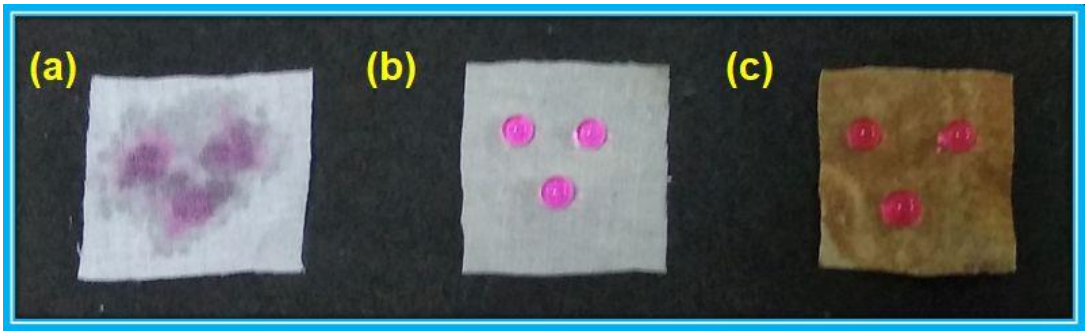

Figure S16. Digital images of water droplets on (a) only polymer coated **SH-MOF**, (b) **SH-MOF′@cotton** composite and (c) **Ag@SH-MOF′@cotton** composite.

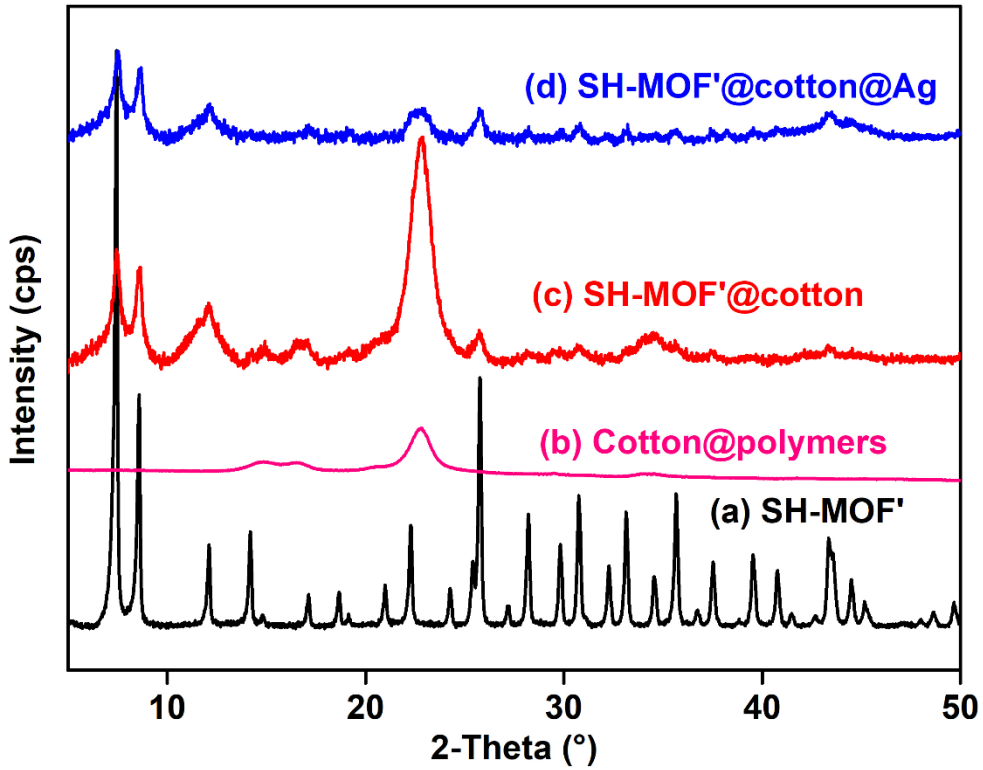

Figure S17. PXRD patterns of (a) **SH-MOF′**, (b) **cotton@polymers**, (c) **SH-MOF′@cotton** composite and (d) **Ag@SH-MOF′@cotton** composite.

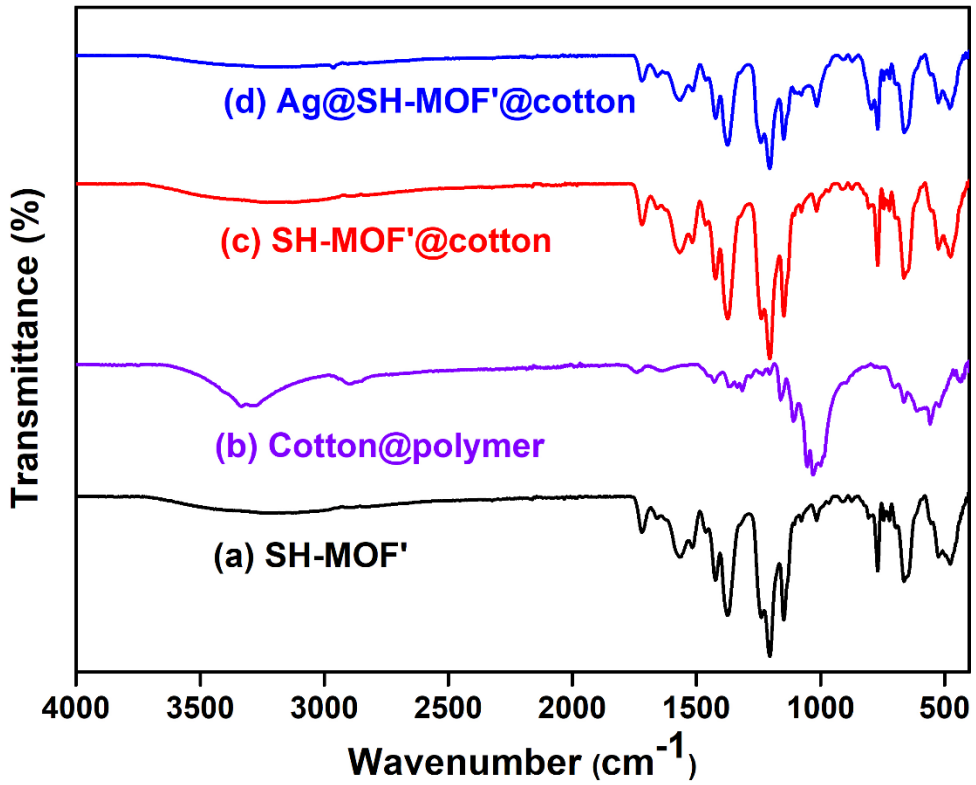

Figure S18. ATR-IR spectra of (a) **Cotton@polymers**, (b) **SH-MOF′**, and (c) **SH-MOF′@cotton** composite.

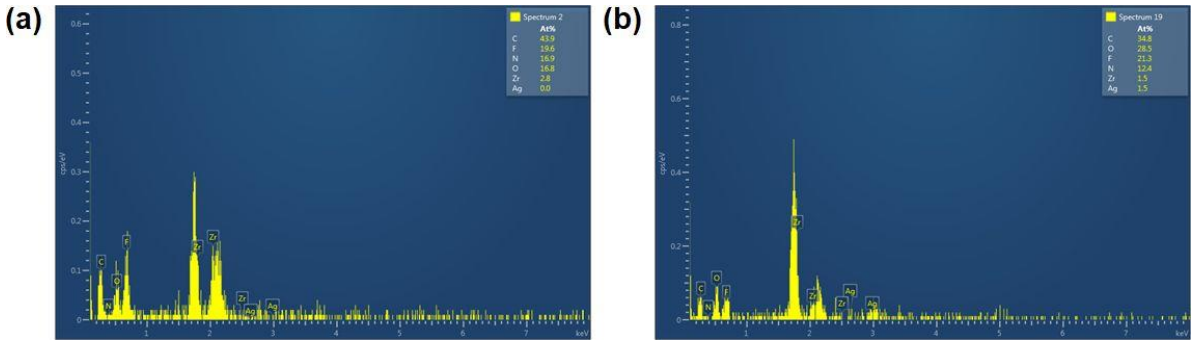

Figure S19. EDX spectrum of (a) **SH-MOF′@cotton** composite and (b) **SH-MOF′@cotton@Ag** composite.

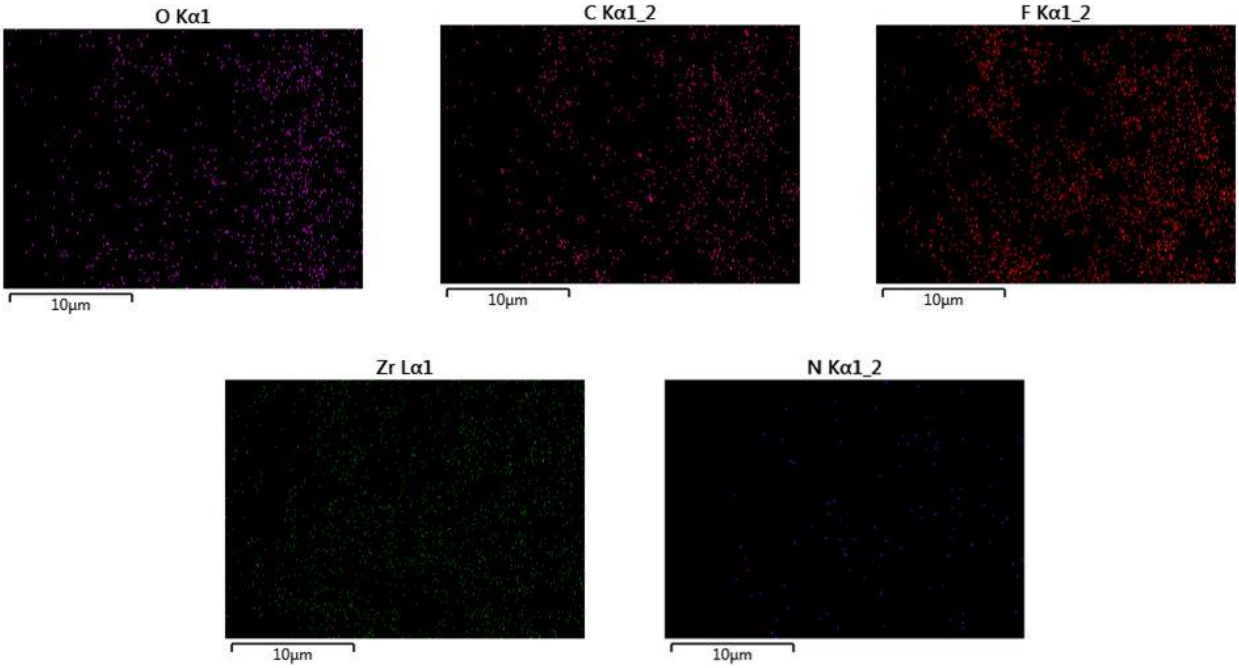

Figure S20. EDX elemental mapping of **SH-MOF′@cotton** composite.

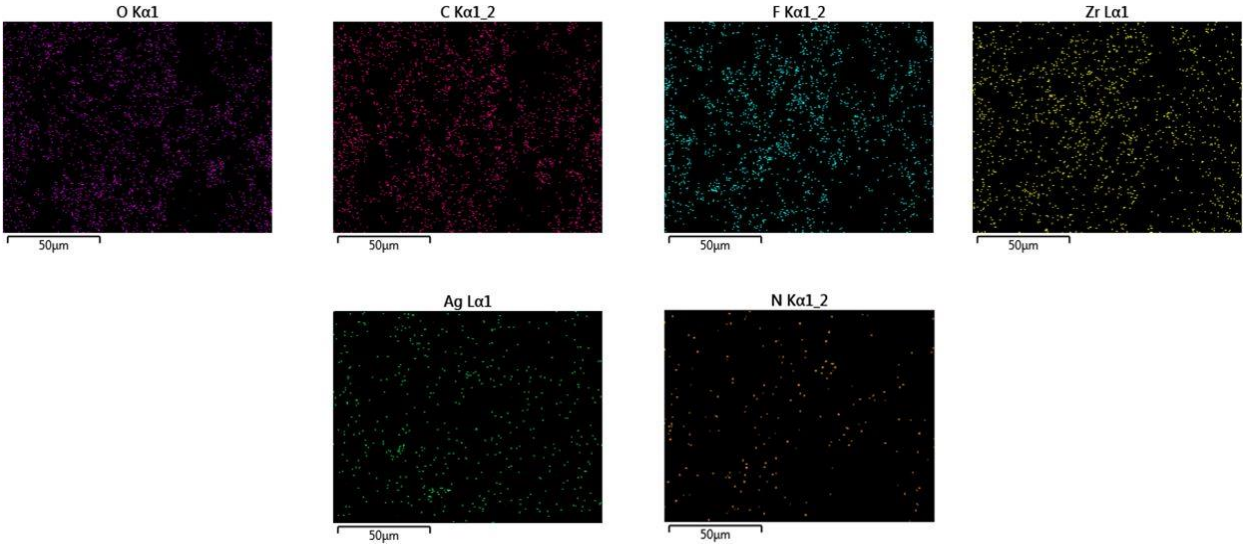

Figure S21. EDX elemental mapping of **SH-MOF′@cotton@Ag** composite.

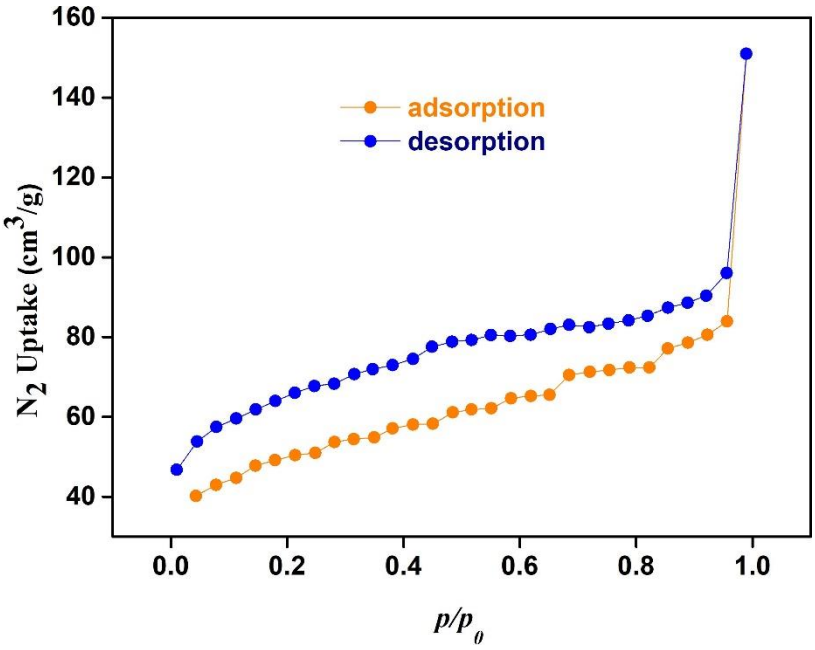

Figure S22. Nitrogen adsorption and desorption isotherms of **SH-MOF′@cotton** composite recorded at -196 °C.

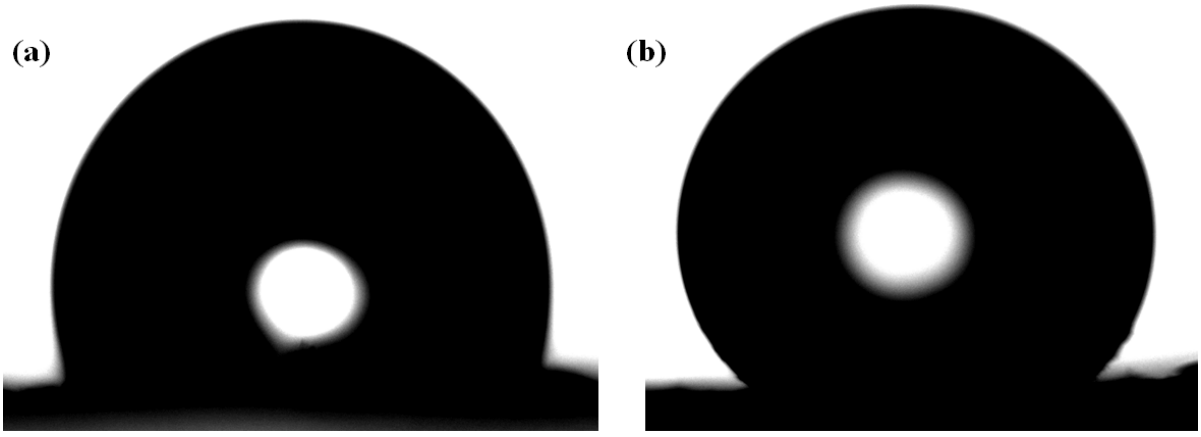

Figure S23. The contact angle image of beaded water droplets on the surface of (a) **polymer@cotton** and (b) **SH-MOF′@cotton@Ag** composite.

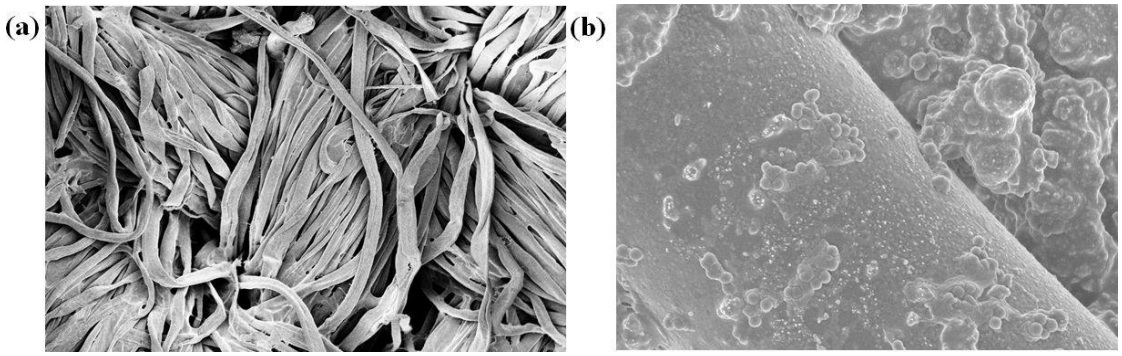

Figure S24. High resolution FE-SEM images of (a) cotton fabric and (b) **SH-MOF′@cotton@Ag** composite.

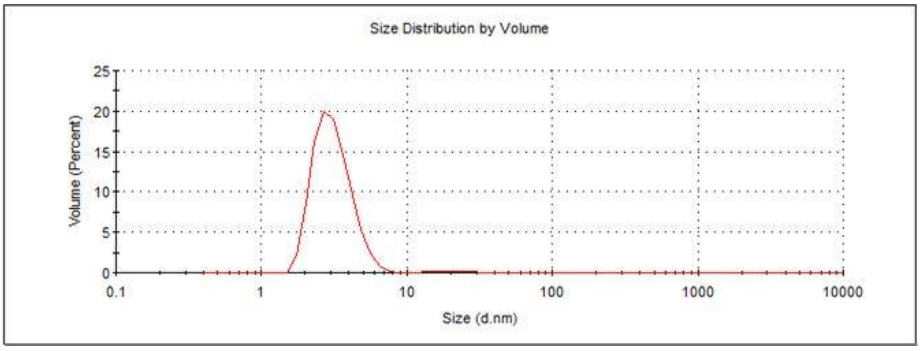

Figure S25. Particle size distribution of the Ag-nano particles measured by DLS method.

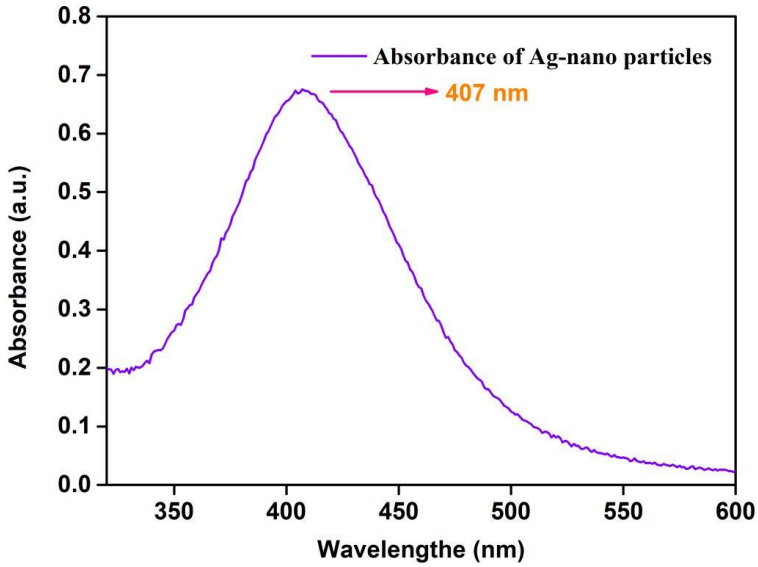

Figure S26. UV-Vis spectrum of Ag-nano particles in aqueous medium.

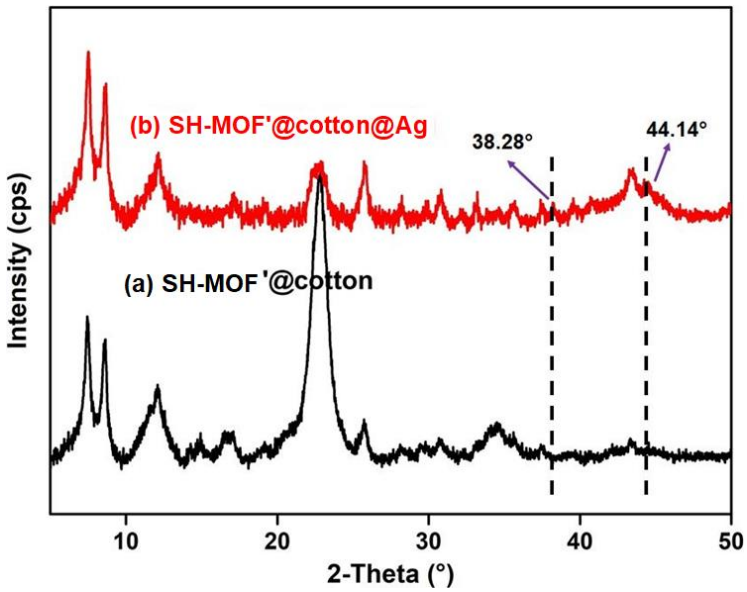

Figure S27. PXRD patterns of (a) **SH-MOF′@cotton** and (b) **SH-MOF′@cotton@Ag** composites.

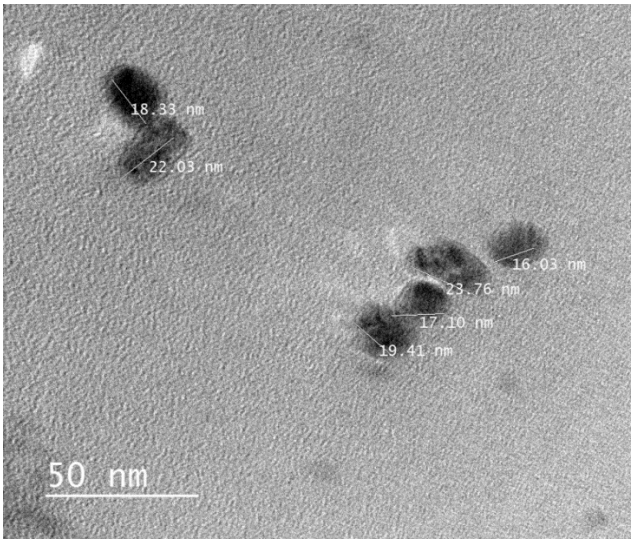

Figure S28. FE-TEM images of Ag nanoparticles.

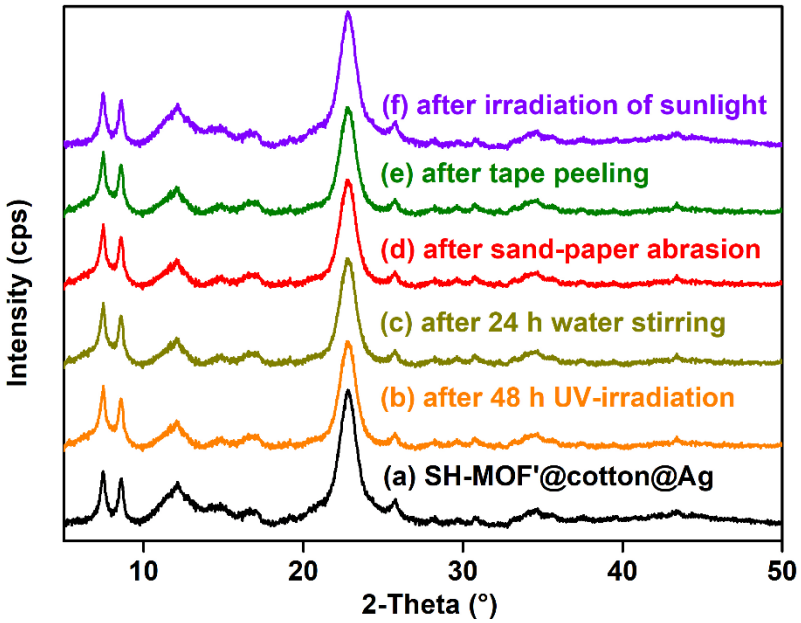

Figure S29. PXRD patterns of (a) **SH-MOF′@cotton@Ag** composite and after (b) UV irradiation for 48 h, (c) stirring in water for 24 h, (d) sand paper abrasion, (e) tape peeling and (f) irradiation of sunlight for 12 h.

Table S2. Water Contact angle (WCA) of **SH-MOF′@cotton@Ag** composite after different mechanical processes.

Conditions	Average WCA (°)
Fresh	153± 1.0
UV irradiation	152 ± 1.2
Water	153 ± 1.5
Sand-paper abrasion	150 ± 1.7
Tape peeling	150 ± 1.0
Irradiation of sunlight	153 ± 1.2

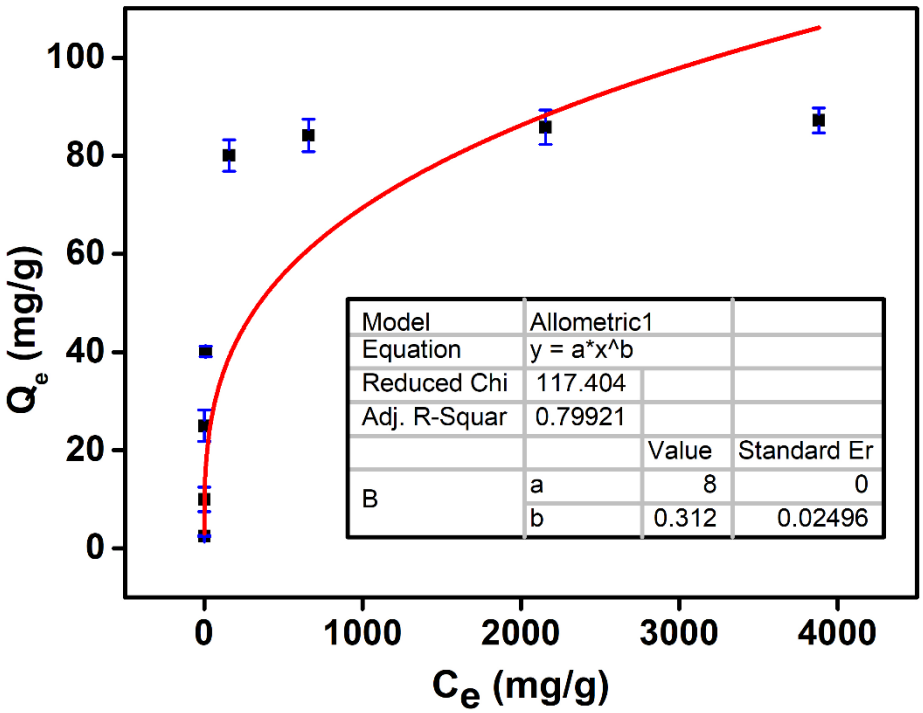

Figure S30. Fitting of absorption results of favipiravir on **SH-MOF′** using the Freundlich model.

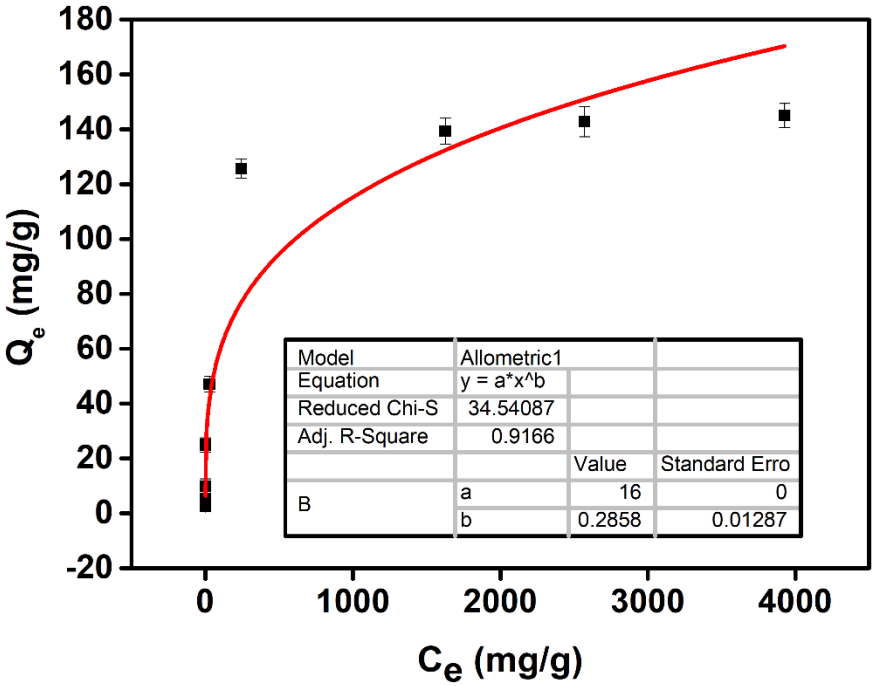

Figure S31. Fitting of absorption results of diflunisal on **SH-MOF′** using the Freundlich model.

Function Group Content and Absorption Capacities of the Drugs Concerning Function Group of the SH-MOF′:

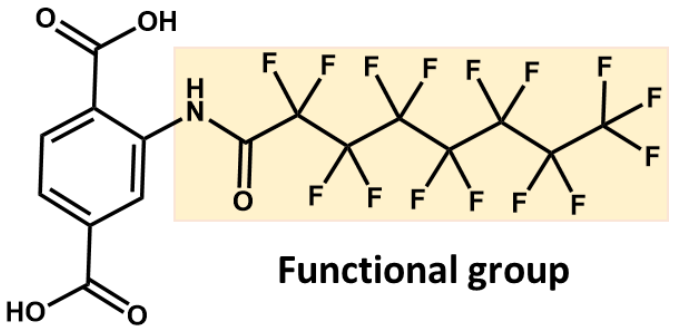

2-(2,2,3,3,4,4,5,5,6,6,7,7,8,8,8-pentadecafluorooctanamido)threphthalic acid linker

Formula of guest-free MOF = $Zr_6(O)_4(OH)_4(C_{16}H_4F_{15}NO_5)_3$
Molecular weight of the MOF = 2404.9 g/mol
Molecular weight of one functional group = 412.9 g/mol
Total molecular weight of the functional groups per unit formula = (412.9 × 3) = 1238.7 g/mol
Fraction of functional groups content in the MOF = 1238.7/2404.9 = 0.53
Adsorption capacity of the MOF for favipiravir = 86.5 mg/g
Adsorption capacity for favipiravir for each functional group = (86.5 × 0.53)/3 = 15.3 mg/g
Adsorption capacity of the MOF for diflunisal = 148 mg/g
Adsorption capacity for diflunisal for each functional group = (148 × 0.53)/3 = 26.1 mg/g

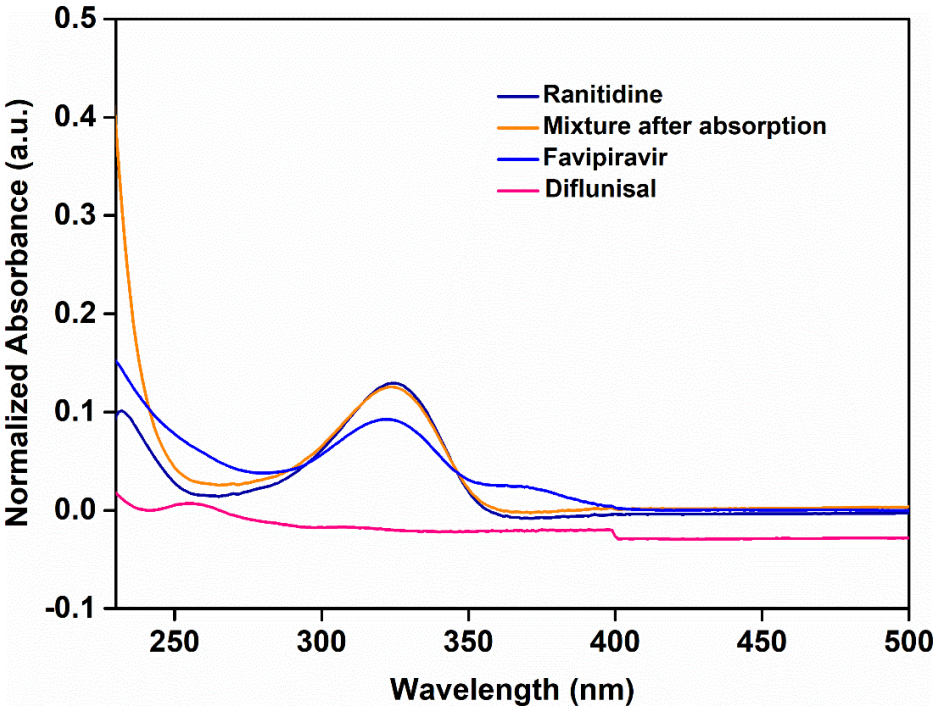

Figure S32. Selective adsorption of water insoluble drugs in presence of water soluble drug ranitidine.

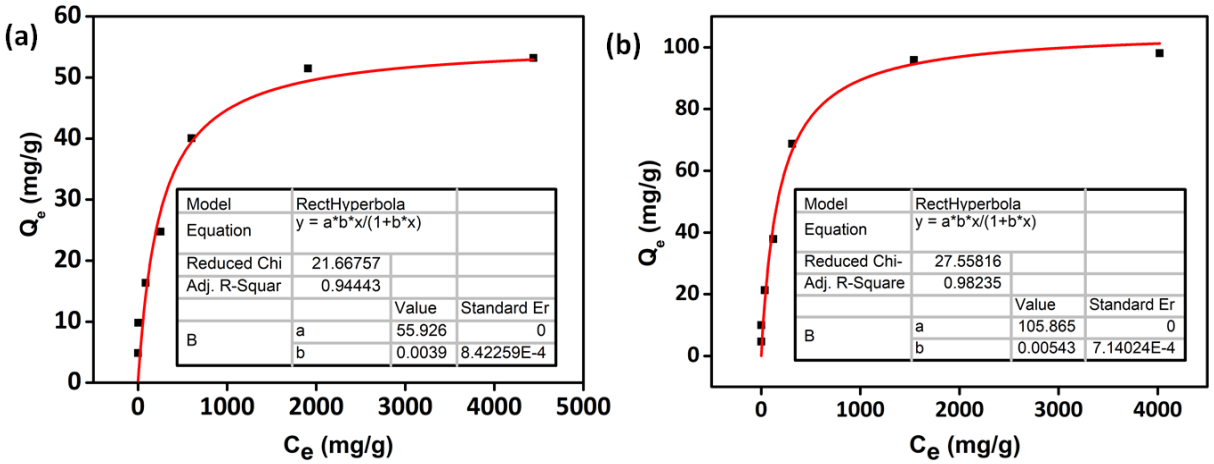

Figure S33. Fitting of adsorption results of (a) favipiravir and (b) diflunisal in **SH-MOF′** using the Langmuir model when both favipiravir and dflunisal are present in equimolar solution.

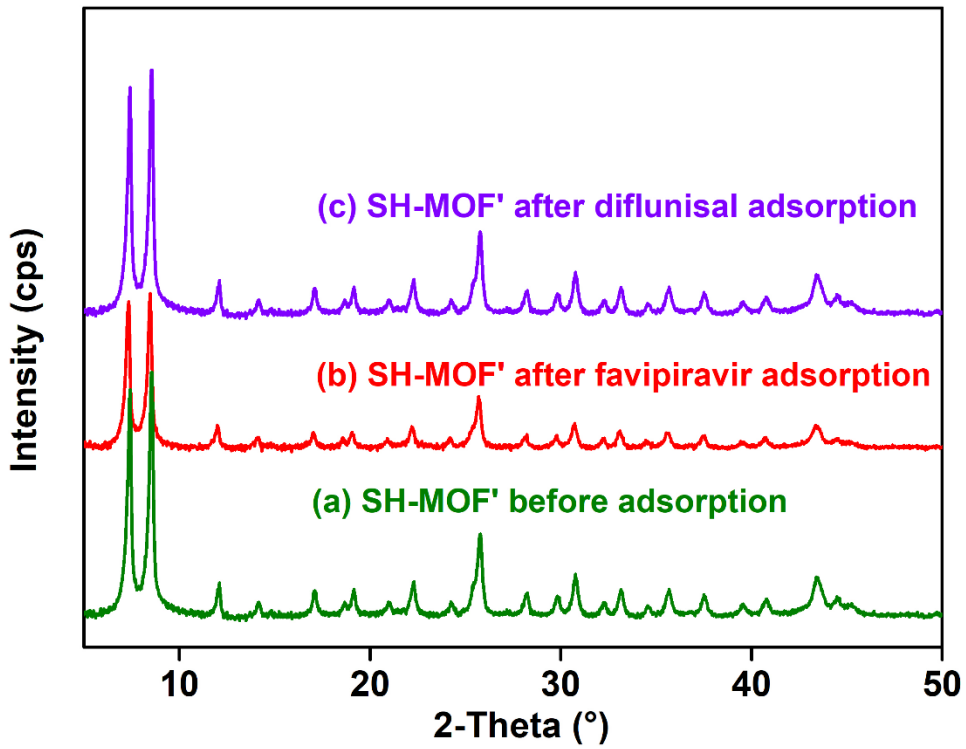

Figure S34. PXRD patterns of **SH-MOF′** before (a) and after favipiravir (b) and diflunisal (c) absorption.

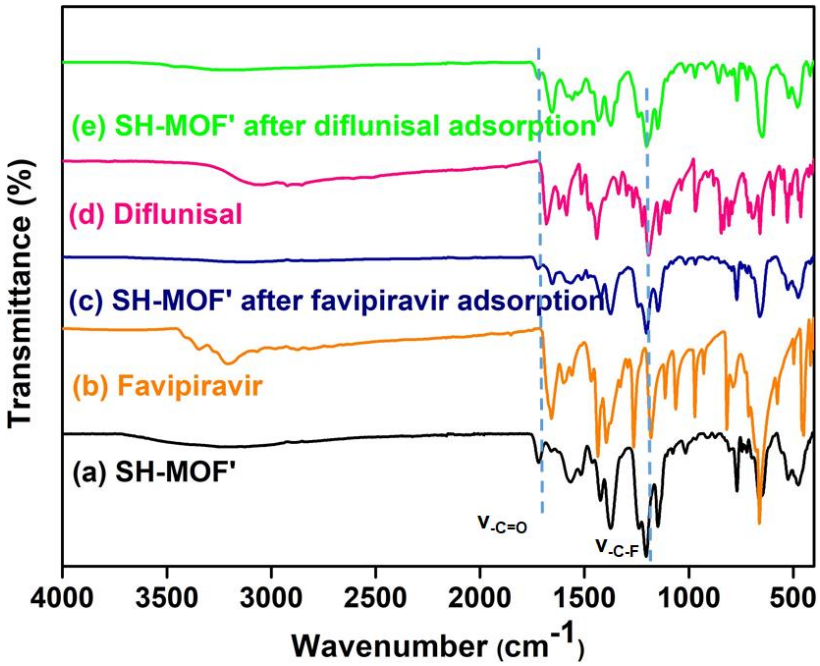

Figure S35. ATR-IR spectra of **SH-MOF′** before (a) and after diflunisal (b) and favipiravir (c) absorption.

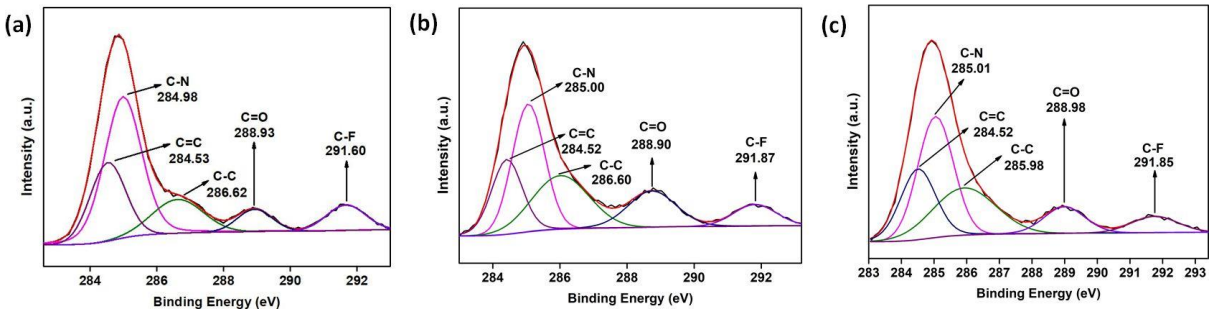

Figure S36. Fitted XPS spectra of C (1s) of **SH-MOF′** before (a) and after favipiravir (b) and diflunisal (c) adsorption.

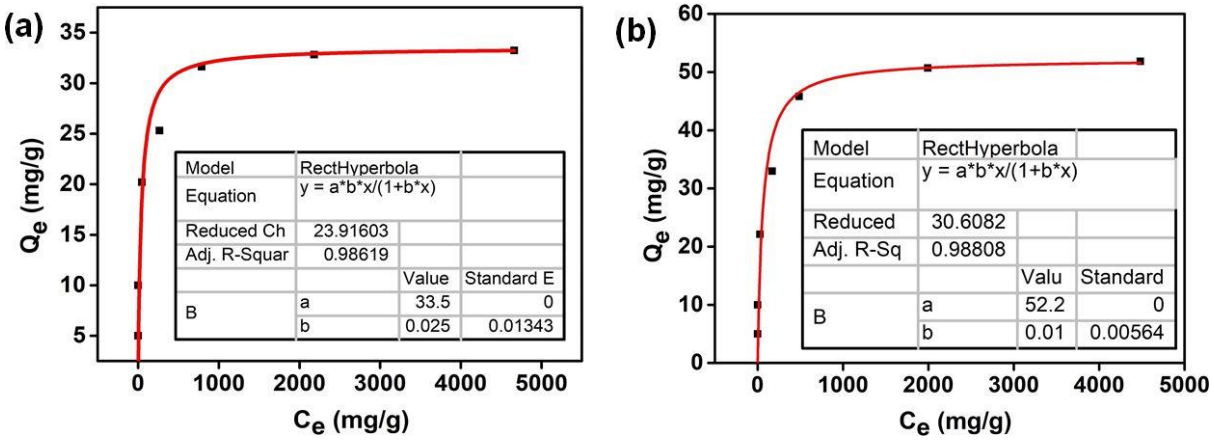

Figure S37. Fitting of adsorption results of (a) favipiravir and (b) diflunisal in Zr-UiO-66 MOF using the Langmuir model.

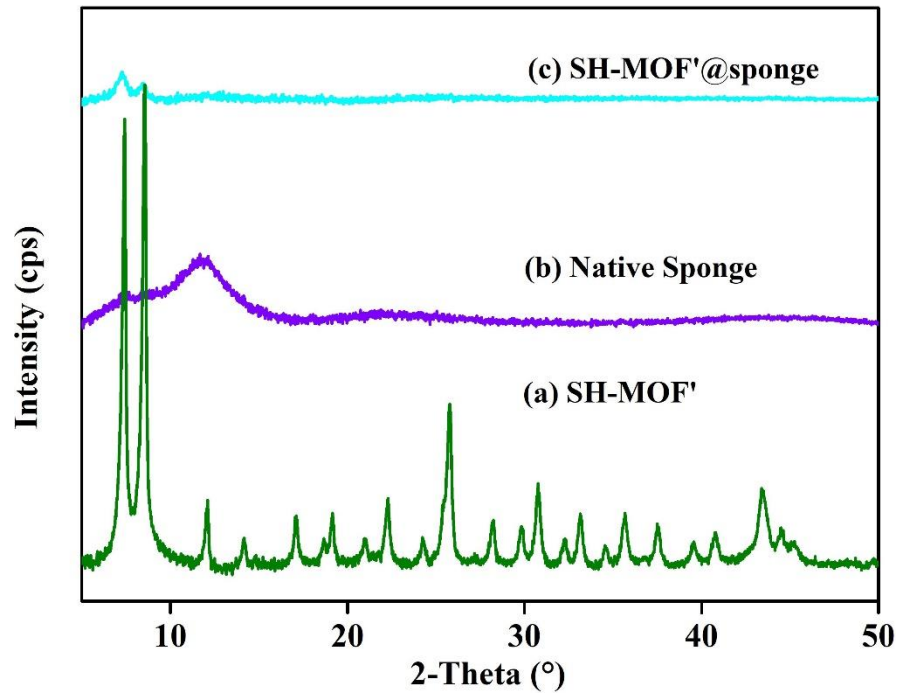

Figure S38. PXRD patterns of (a) **SH-MOF′**, (b) native sponge and (c) **SH-MOF′@sponge** composite.

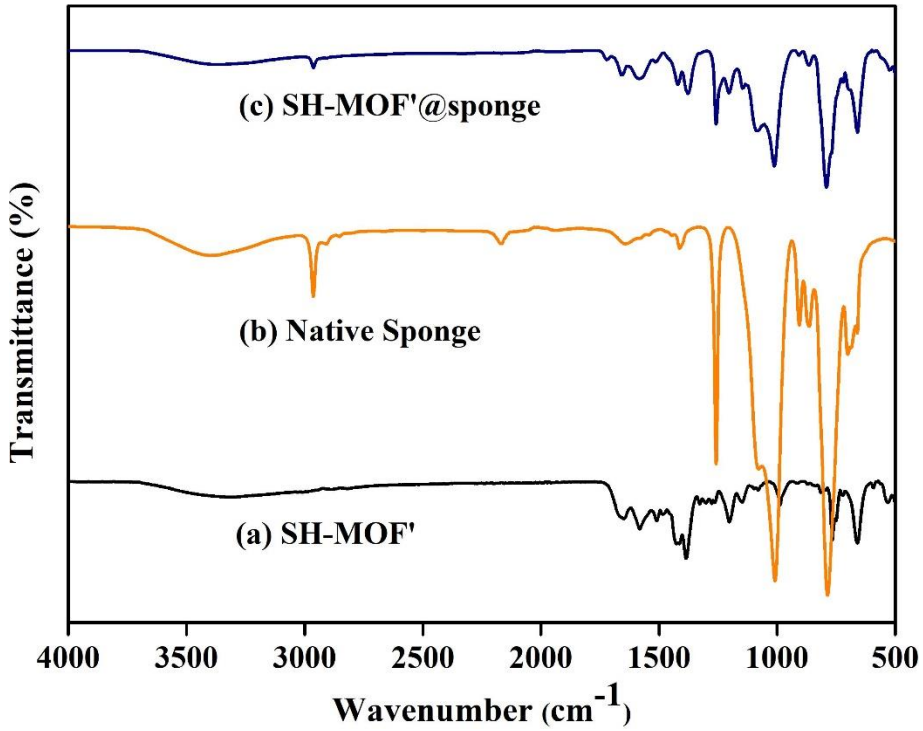

Figure S39. ATR-IR spectra of (a) **SH-MOF′**, (b) native sponge and (c) **SH-MOF′@sponge** composite.

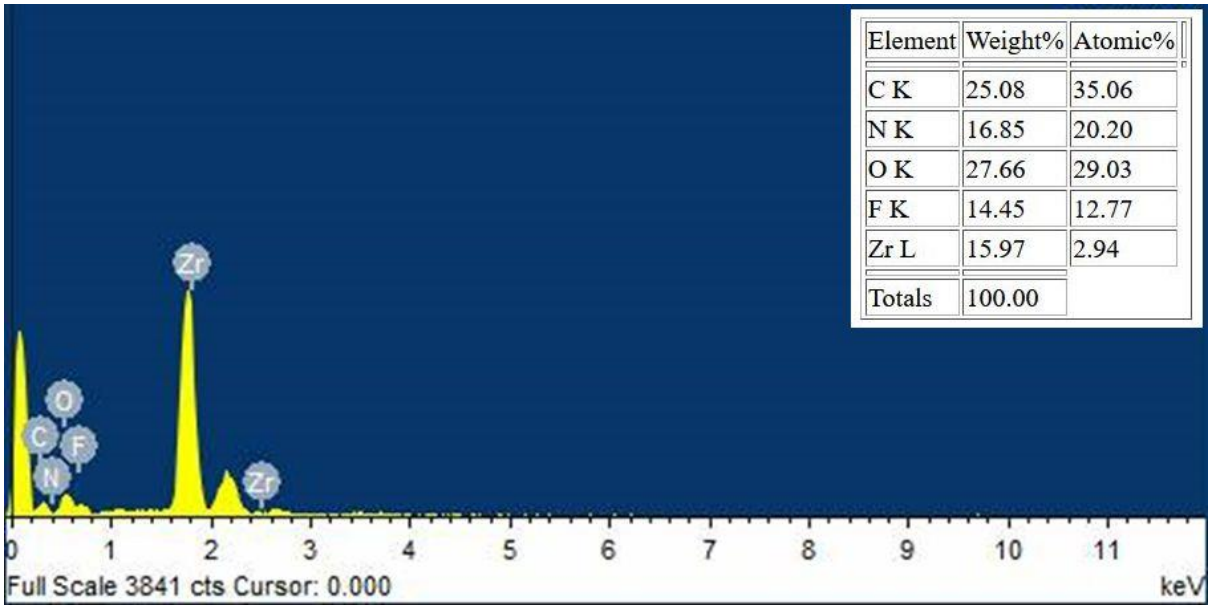

Figure S40. EDX spectrum of **SH-MOF′@sponge** composite.

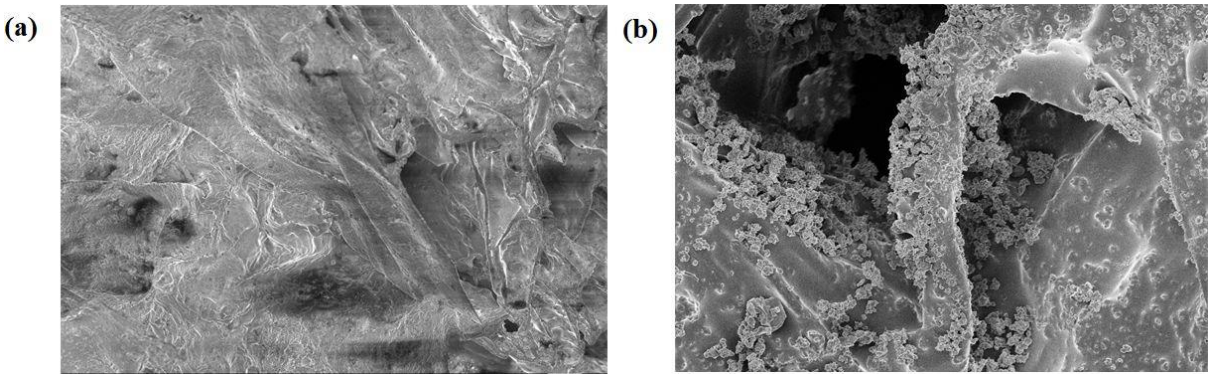

Figure S41. FE-SEM images of (a) navite sponge and **SH-MOF′@sponge** composite.

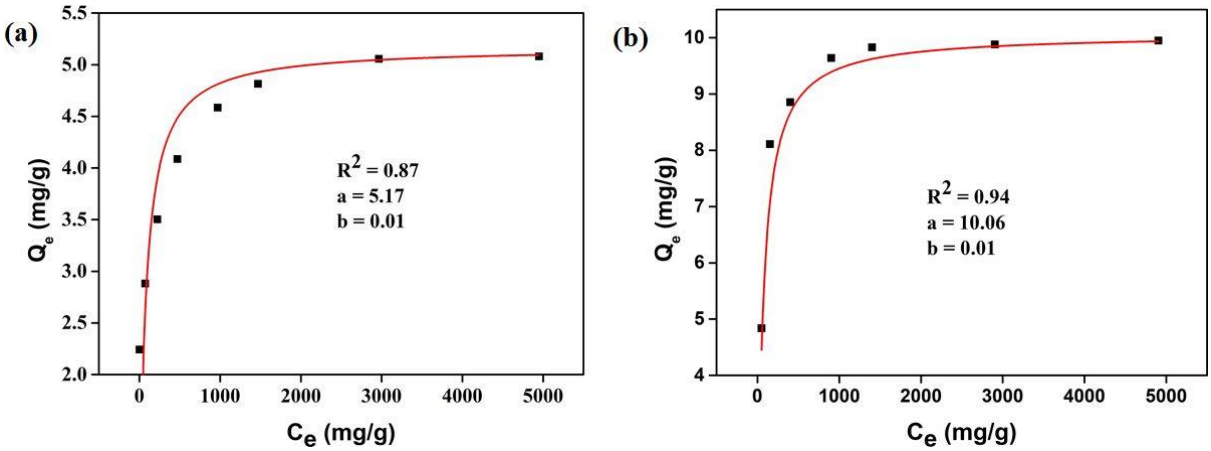

Figure S42. Fitting of adsorption results of (a) favipiravir and (b) diflunisal in native sponge using the Langmuir model.

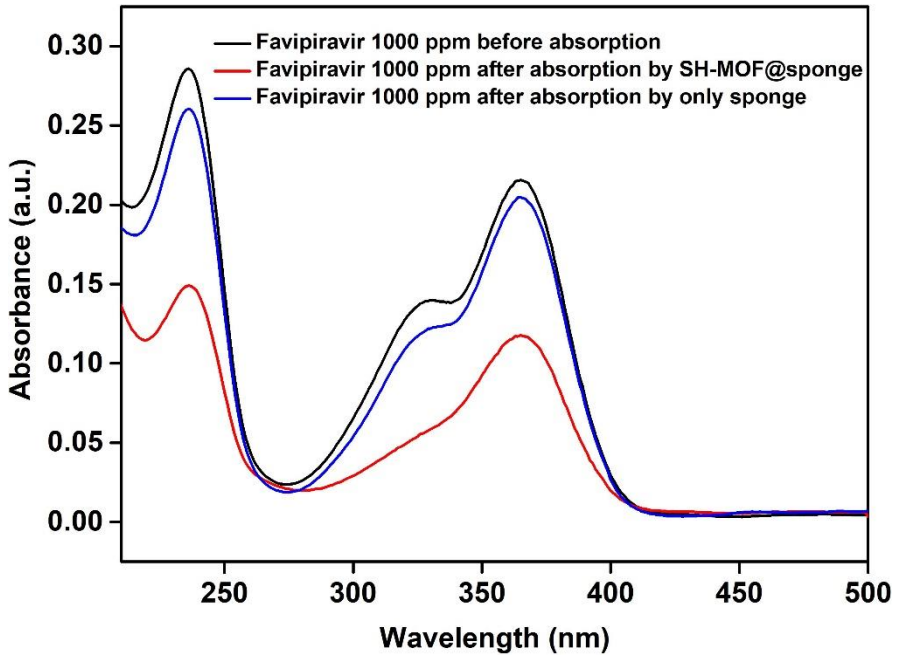

Figure S43. UV-Vis spectra of 10 µL of 1000 ppm favipiravir solution (black), after adsorption by native sponge (blue) and after adsorption by **SH-MOF′@sponge** composite (red).

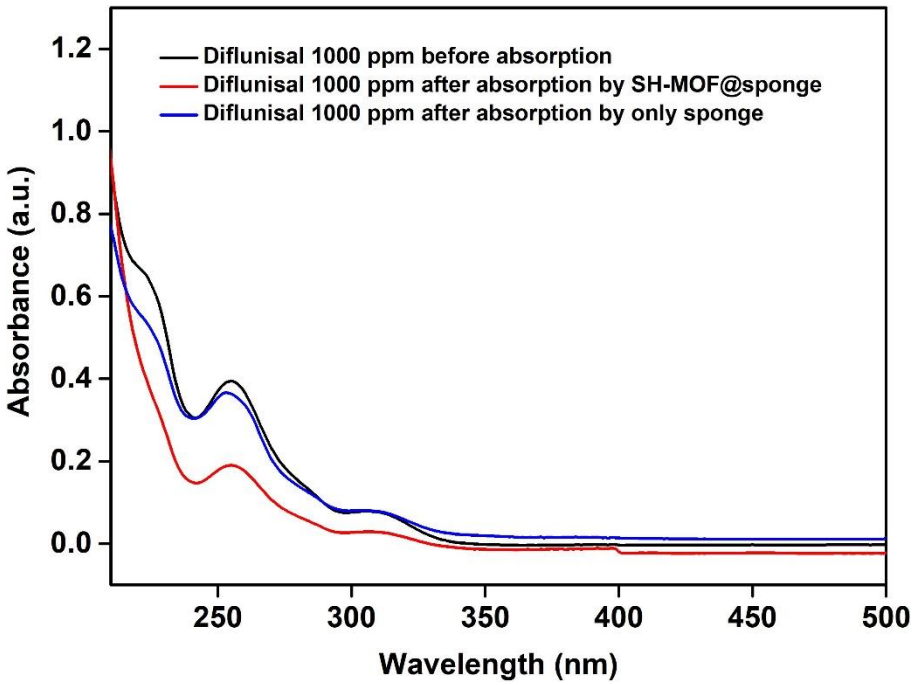

Figure S44. UV-Vis spectra of 10 µL of 1000 ppm favipiravir solution (black), after adsorption by native sponge (blue) and after adsorption by **SH-MOF′@sponge** composite (red).

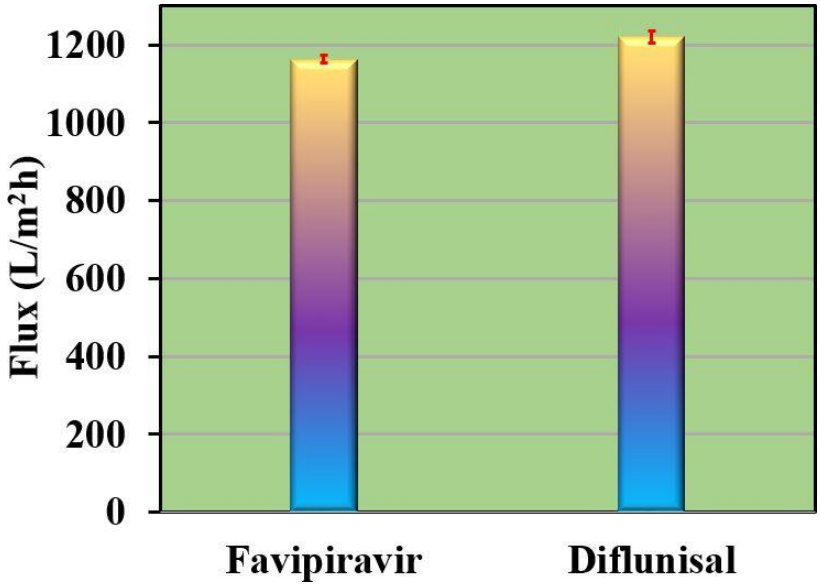

Figure S45. Flux of separation of drugs by **SH-MOF′@sponge** composite.

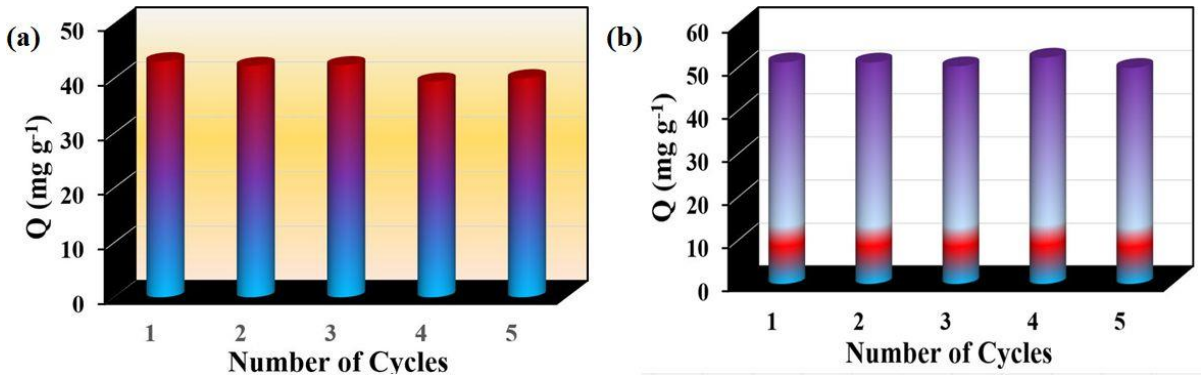

Figure S46. Reusability of the **SH-MOF′@sponge** composite for the separation of (a) favipiravir and (b) diflunisal.

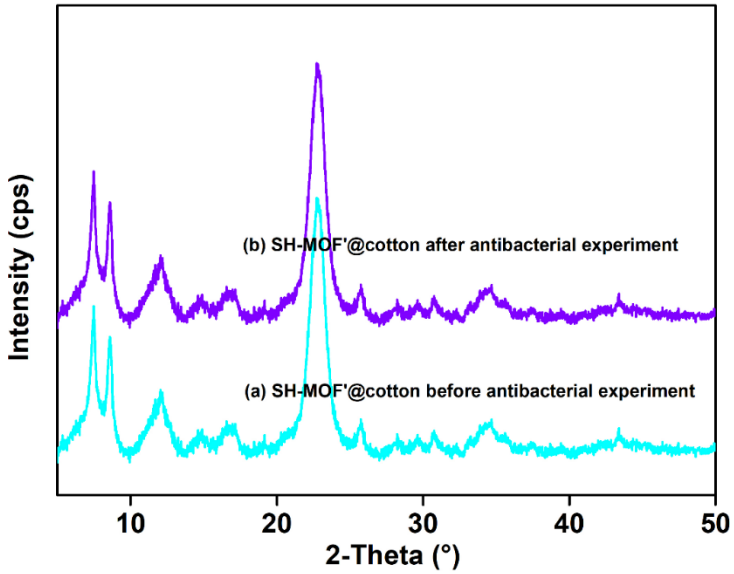

Figure S47. PXRD patterns of **SH-MOF′@cotton** composite (a) before and (b) after bacterial anti-adhesion (model bacteria: *Staphylococcus aureus* (MTCC-96)).

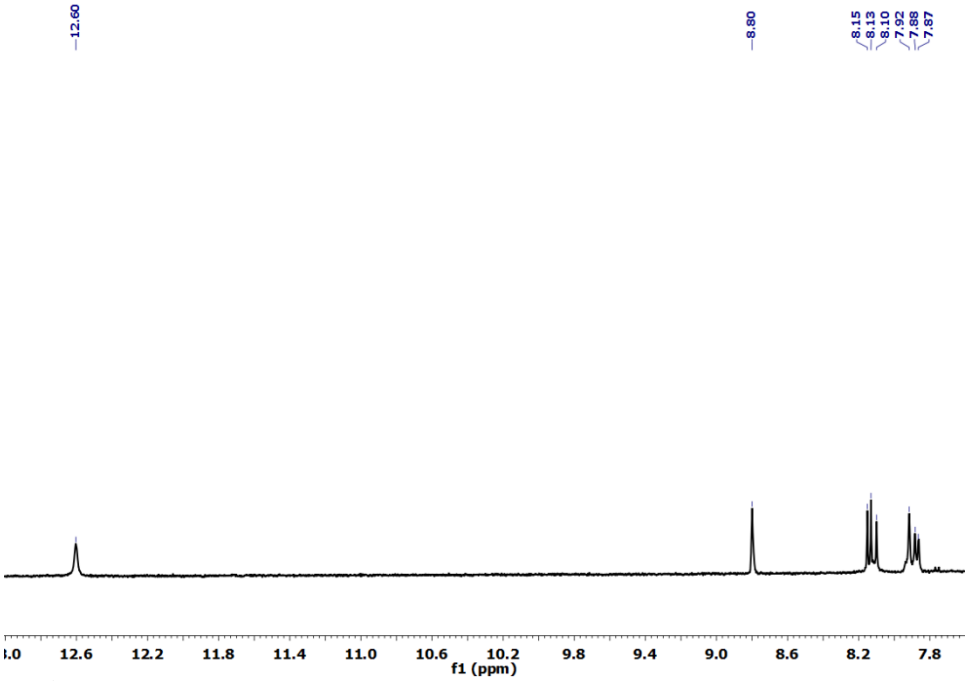

Figure S48. ^{1}H NMR spectrum of **SH-MOF′** digested in DMSO-d_6 (digested by 40% HF).

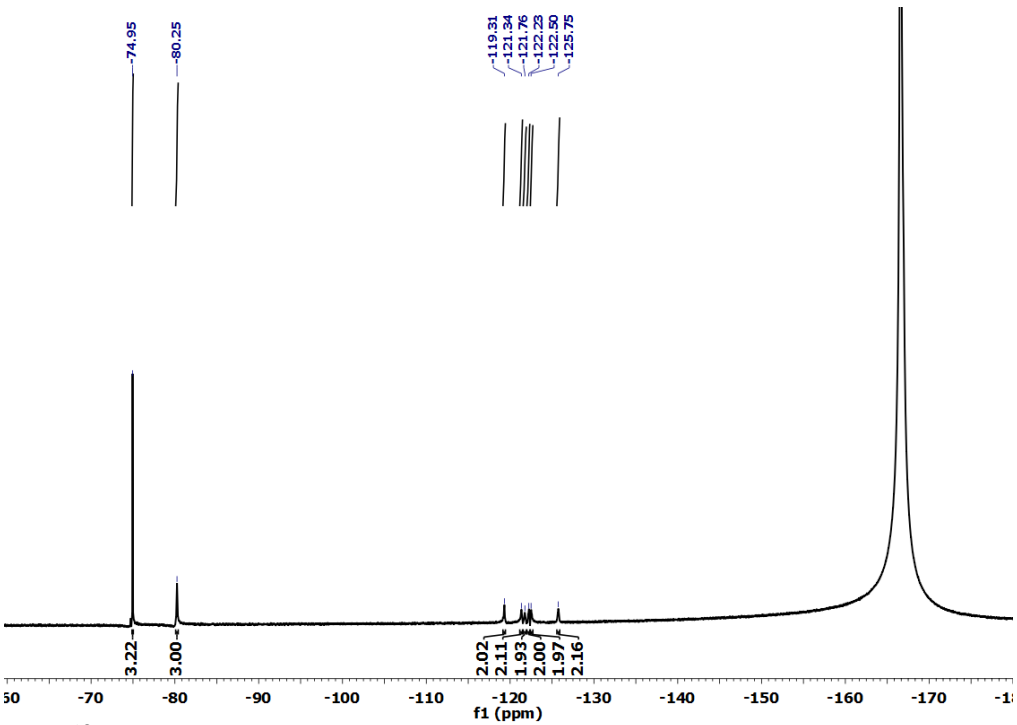

Figure S49. ^{19}F NMR spectrum of **SH-MOF′** digested in DMSO-d_6 (digested by 40% HF).

Table S3. Unit cell parameters of **SH-MOF′** obtained by indexing its PXRD data. The obtained values have been compared with parent UiO-66 MOF.

Compound Name	**SH-MOF′**	UiO-66[1]
Crystal System	cubic	cubic
a = b = c (Å)	20.707(3)	20.700(2)
V ($Å^3$)	8878.7(23)	8869.7(2)

Reference:

(1) Cavka, J. H.; Jakobsen, S.; Olsbye, U.; Guillou, N.; Lamberti, C.; Bordiga, S.; Lillerud, K. P. A new zirconium inorganic building brick forming metal organic frameworks with exceptional stability. *J. Am. Chem. Soc.* **2008,** *130* (42), 13850-13851.